Planetary and Space Science 191 (2020) 105021

Contents lists available at ScienceDirect

Planetary and Space Science

journal homepage: www.elsevier.com/locate/pss

Incision of Ma'adim Vallis (Mars) by dry volcanic megafloods effused from multiple highland sources

David W. Leverington

Department of Geosciences, Texas Tech University, Lubbock, TX, 79409, USA

A B S T R A C T

The Ma'adim Vallis channel system extends ~900 km northward across the highlands of Terra Cimmeria into Gusev crater. Formation of this system has previously been attributed to the past operation of aqueous processes variously involving periodic surface runoff from adjacent intercrater plains, releases from one or more highland lakes, sudden and voluminous effusions of groundwater, and/or basal sapping. Some researchers have interpreted Ma'adim Vallis as a product of multiple discrete episodes of highland water flow that collectively occurred over a broad time frame extending from the Noachian to the Amazonian, but others have favored catastrophic development of the system as a result of the partial drainage of a long-lived lake hypothesized to have existed in the Eridania basin in the Late Noachian. Problematically, clear geomorphological and mineralogical evidence is lacking for the past voluminous flow of water along Ma'adim Vallis, and for the existence of one or more long-lived water bodies in adjacent highlands. Instead, the properties of Ma'adim Vallis suggest dry volcanic origins involving effusions of low-viscosity flood lavas from multiple highland sources during the Noachian and Hesperian. The geochemistry of lavas accumulated near the mouth of Ma'adim Vallis suggests viscosities sufficiently low to have allowed for substantial incision into bedrock substrates if lavas were erupted at high effusion rates and with high total volumes. Formation of Ma'adim Vallis is estimated to have required effusion of a minimum lava volume of ~112,000 km^3. Development of many other highland channel networks on Mars is expected to have involved analogous volcanic processes.

1. Introduction

Ma'adim Vallis is a Martian channel system that is located in the highlands of Terra Cimmeria and terminates at Gusev crater (Milton, 1973; Sharp and Malin, 1975; Baker, 1982; Schneeberger, 1989; Goldspiel and Squyres, 1991; Cabrol et al., 1996, 1998ab; Carr, 1996; Kuzmin et al., 2000; Aharonson et al., 2002; Irwin et al., 2002, 2004) (Figs. 1 to 3). The main channel has typical widths of ~8–15 km but widens to ~25 km near its mouth (e.g., Sharp and Malin, 1975; Schneeberger, 1989; Irwin et al., 2002). The system is characterized by geomorphic features such as terraces, inner channels, and immature and theater-headed tributary valleys (e.g., Schneeberger, 1989; Cabrol et al., 1998a,b; Gulick, 2001; Aharonson et al., 2002). Initial formation of Ma'adim Vallis is believed to have taken place at the end of the Noachian, with some additional development possibly taking place in the Hesperian and Amazonian (e.g., Cabrol et al., 1998a; Irwin et al., 2004).

Ma'adim Vallis has been widely interpreted as a product of aqueous processes involving surface runoff from adjacent plains, overflow from one or more large lakes, catastrophic effusions of groundwater, and/or groundwater sapping (e.g., Sharp and Malin, 1975; Cabrol et al., 1998a; Irwin et al., 2002, 2004; Fassett and Head, 2008; Baker and Head, 2012). Aqueous interpretations of this system have suggested earlier warm and wet conditions on Mars and the possible occurrence of precipitation (e.g., Goldspiel and Squyres, 1991; Cabrol and Grin, 2001; Irwin et al., 2002), and have highlighted the potential exobiological importance of component channels, the system terminus at Gusev crater, and associated basins of the southern highlands (e.g., Landheim et al., 1994; Cabrol et al., 1994, 1996, 1998a,b; Grin and Cabrol, 1997; Kuzmin et al., 2000; de Pablo and Fairén, 2004; Davila et al., 2011).

In contrast with earlier perspectives, it is now apparent that Ma'adim Vallis lacks the clear sedimentary and geochemical signatures expected of formation as an aqueous system, and instead has properties consistent with dry volcanic origins involving the eruption of low-viscosity lavas from multiple highland sources. The purpose of this paper is to introduce a volcanic interpretation of Ma'adim Vallis, and to present estimates of possible flow conditions and the minimum volume of lava required to form the system. The implications of volcanic origins for our understanding of the nature and history of Mars are explored.

2. Overview of the Ma'adim Vallis channel system

The Ma'adim Vallis channel system extends ~900 km northward across the highlands of Terra Cimmeria into Gusev crater (Figs. 1 to 5). The system has an average longitudinal gradient of ~0.13°, with component channels and valleys characterized along many reaches by steep walls and flat floors, and with typical channel depths of ~700

E-mail address: david.leverington@ttu.edu.

https://doi.org/10.1016/j.pss.2020.105021
Received 11 January 2020; Received in revised form 6 June 2020; Accepted 7 June 2020
Available online 26 June 2020

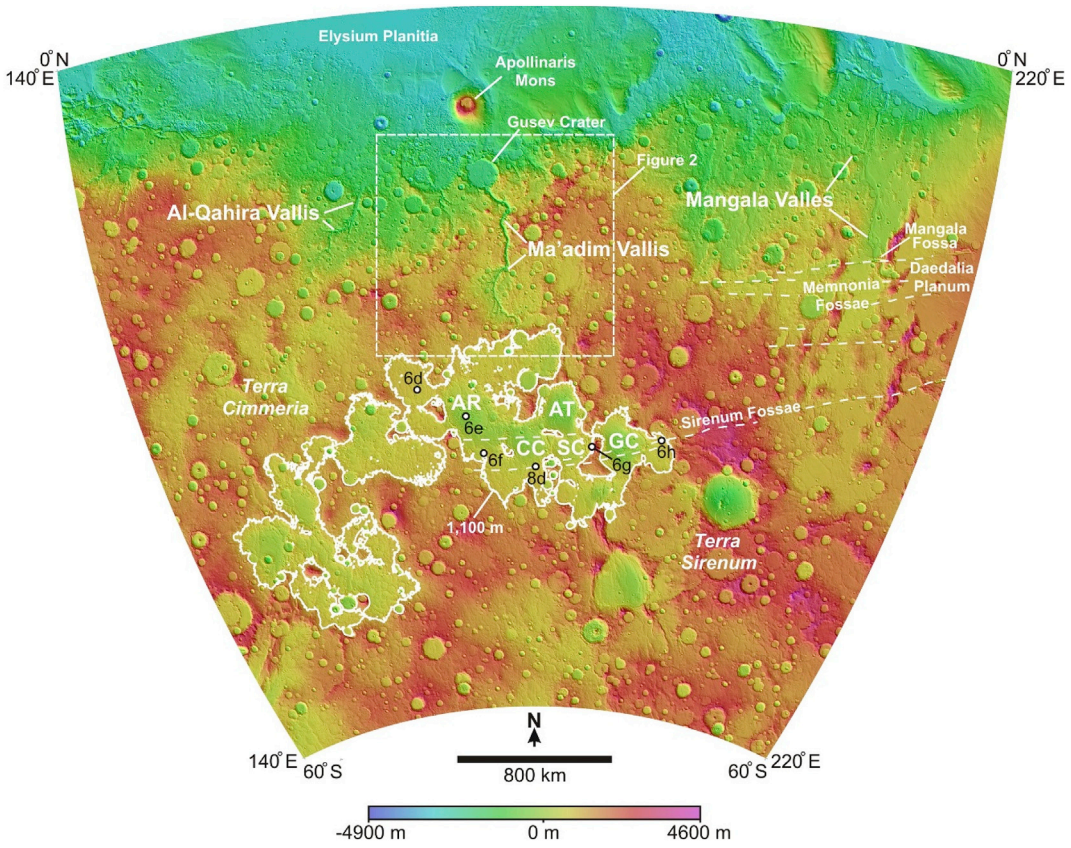

Fig. 1. Topography and shaded relief of the Ma'adim Vallis and Eridania basin region. The1,100 m contour that defines the main extent of a lake previously hypothesized to have existed within the Eridania basin is given. Large fields of flat-topped mesas and rounded knobs located along the floors of impact basins, named after their associated basins, include: *AR*: Ariadnes Colles; *AT*: Atlantis Chaos; *GC*: Gorgonum Chaos; *CC*: Caralis Chaos; *SC*: Simois Colles. The locations of selected areas depicted in Fig. 6 and 8 are given. Mars Orbiter Laser Altimeter (MOLA) data after Smith et al. (2003). Lambert azimuthal equal-area projection.

m–2300 m below adjacent highlands (e.g., Schneeberger, 1989; Goldspiel and Squyres, 1991; Cabrol and Grin, 1998a; Irwin et al., 2002, 2004). An inner channel is incised into terraces that are present along some system reaches, which has suggested multiple episodes of system development (e.g., Goldspiel and Squyres, 1991; Landheim et al., 1994; Cabrol et al., 1996; Kuzmin et al., 2000) (Fig. 6b). Tributary valleys to the main Ma'adim Vallis channel are relatively short and immature (Fig. 6a), with convex-up longitudinal profiles, and in some cases have abrupt theater-shaped heads (e.g., Cabrol et al., 1998a; Gulick, 2001; Aharonson et al., 2002; Irwin et al., 2004). Adjacent highland plateaus of Terra Cimmeria and Terra Sirenum are predominantly comprised of cratered and dissected terrains of Noachian age that show evidence for multiple periods of resurfacing in the Noachian, Hesperian, and Amazonian (e.g., Scott and Tanaka, 1986; Greeley and Guest, 1987; Goldspiel and Squyres, 1991; Baker and Head, 2012; Molina et al., 2014; Tanaka et al., 2014; Adeli et al., 2015; Brož et al., 2015; Pajola et al., 2016; Michalski et al., 2017) (Fig. 4a). Much of the main Ma'adim Vallis channel has relatively flat floors (Fig. 7) that are ridged in places. Ma'adim Vallis enters Gusev crater through a breach in its southern rim, and a separate breach opens northwestward toward the northern lowlands, suggesting past flow into and beyond Gusev crater (e.g., Schneeberger, 1989; Goldspiel and Squyres, 1991; Scott and Chapman, 1995; Kuzmin et al., 2000). Prominent volcanic cones in the vicinity of Ma'adim Vallis include Apollinaris Mons in the Elysium region to the north (Fig. 1) and Apollinaris Tholus and Zephyria Tholus in the highlands of Terra Cimmeria to the west (Figs. 2 and 3). Estimates of thermal inertia (Fig. 4b) indicate that the Ma'adim Vallis channel system is partly mantled by fines that can obscure underlying rock, especially along the middle and northern reaches of the system (e.g., Putzig et al., 2005; Edwards et al., 2009); along Ma'adim Vallis itself and at adjacent highlands, typical thermal inertia values derived from data collected by the Thermal Emission Spectrometer (TES) range from ~150 to 240 tiu (Christensen and Fergason, 2013), suggesting that mantling deposits composed of sand-sized or smaller particles should be especially common here (e.g., Putzig and Mellon, 2007). The volume of material eroded to form Ma'adim Vallis and its tributaries is ~14,000 km^3 (e.g., Goldspiel and Squyres, 1991; Cabrol et al., 1996; Gulick, 2001; Irwin et al., 2002, 2004; Luo et al., 2015).

Gusev crater is an ~160-km-wide impact feature that has a relatively degraded rim and is extensively mantled by units that form plains that are ridged in places (e.g., Landheim et al., 1994; Cabrol et al., 1998b; Kuzmin et al., 2000) (Figs. 2, 3 and 6c). Two 30-km-wide impact craters are superimposed upon the southern rim of Gusev crater, and are themselves breached where Ma'adim Vallis enters from the south (e.g., Landheim et al., 1994; Cabrol et al., 1998b). Prominent terraces exist along the inner margins of parts of Gusev crater and are separated by lower-elevation plains, and fields of isolated mounds and mesas exist in the southern part of the crater near the mouth of Ma'adim Vallis (e.g., Landheim et al., 1994; Grin and Cabrol, 1997; Cabrol et al., 1998b; Kuzmin et al., 2000). The inner rim of Gusev crater is crossed in places by small channels and valleys, and accumulations of mass-wasted materials are present along the crater floor adjacent to the inner rim (e.g., Landheim et al., 1994; Cabrol et al., 1998b; Kuzmin et al., 2000). Immediately north of Gusev crater, plains units are partly mantled by deposits including those of the Medusae Fossae Formation (e.g., Scott and Tanaka, 1986; Kuzmin et al., 2000; Tanaka et al., 2014; Chuang et al., 2019).

Gusev crater was visited by the Spirit rover and found to be extensively mantled by Hesperian-aged volcanic flows (e.g., Grant et al., 2004; Golombek et al., 2005; Greeley et al., 2005) of a relatively pristine mineralogical character that is indicative of little hydrous alteration (e.g., Squyres et al., 2004; Haskin et al., 2005; Morris et al., 2006; Mittlefehldt

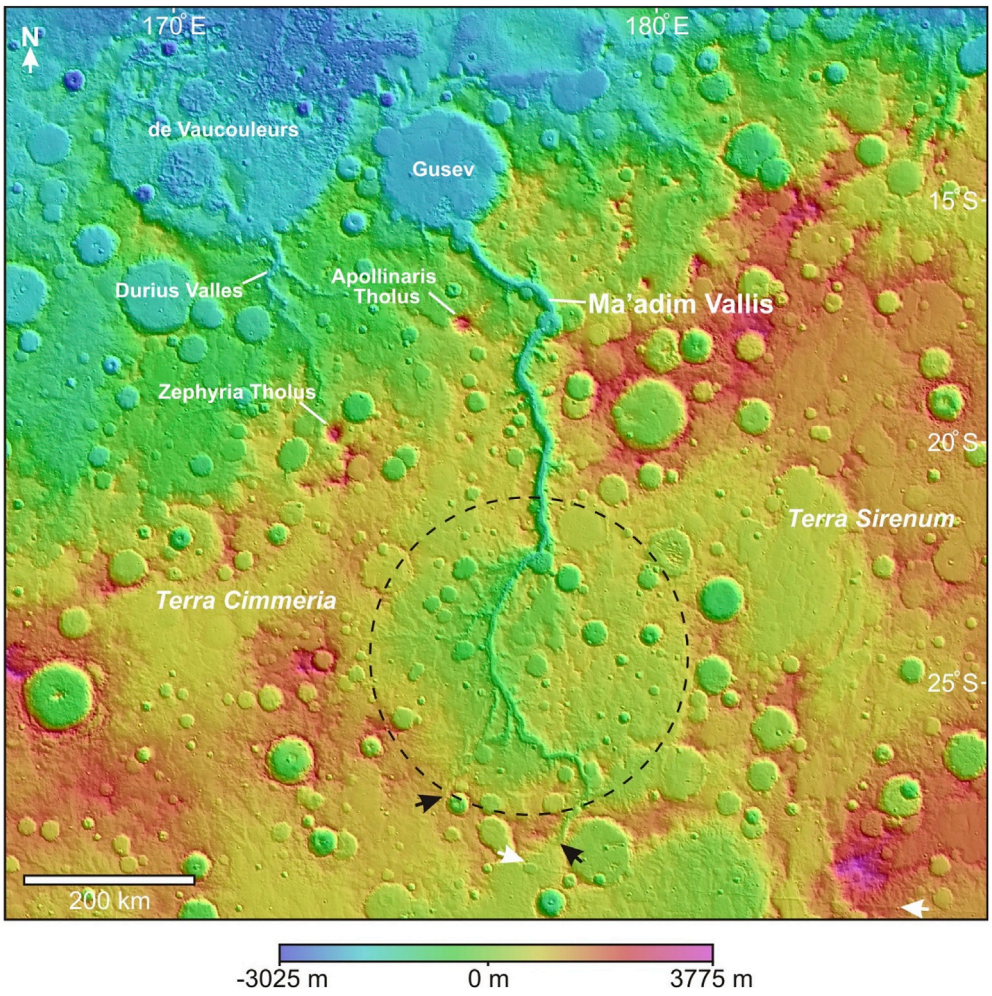

Fig. 2. Topography and shaded relief of the Ma'adim Vallis region. The "Intermediate basin" of Irwin et al. (2002, 2004) is depicted (dashed circle), as are the heads of two southern channels (black arrows). An example of an east-west oriented graben-like structure located near the head of Ma'adim Vallis is indicated by white arrows at bottom-right. MOLA topographic data after Smith et al. (2003). Lambert azimuthal equal-area projection.

et al., 2019). No sedimentary deposits of obvious lacustrine origin were identified in data collected by the Spirit rover (e.g., Squyres et al., 2004), though orbital data indicate that localized exposures of hydrated minerals such as phyllosilicates are associated with some plains units (e.g., Carter and Poulet, 2012). Noachian-aged outcrops visited by Spirit at the Columbia Hills, which rise above adjacent Hesperian plains of Gusev crater, contain materials in places that were moderately to pervasively altered under low water-to-rock ratios, locally forming carbonates, sulfates, oxides, phosphates, halides, clays, and amorphous silica (e.g., Yen et al., 2008; Ming et al., 2006; Squyres et al., 2006, 2008; Morris et al., 2006, 2010; Carter and Poulet, 2012; Mittlefehldt et al., 2019).

The southernmost limits of the Ma'adim Vallis system are demarcated by the upper reaches of two channels that commence full-born at gaps in the northern divide of a large topographic basin (the "Eridania basin") that extends across the highlands of Terra Cimmeria and Terra Sirenum (e.g., Irwin et al., 2002, 2004; Fassett and Head, 2008; Goudge et al., 2018) (Figs. 1 to 3). As with highlands to the north, the Eridania basin is comprised in part of numerous highly degraded impact craters of Noachian age and is largely mantled by plains units that are ridged in places and that were deposited in the Noachian, Hesperian, and Amazonian (e.g., Tanaka, 1986; Scott and Tanaka, 1986; Greeley and Guest, 1987; Hartmann et al., 2001; Irwin et al., 2004, 2013; Goudge et al., 2012; Baker and Head, 2009, 2012; Molina et al., 2014; Tanaka et al., 2014; Adeli et al., 2015; Brož et al., 2015; Pajola et al., 2016; Michalski et al., 2017) (Fig. 6d). Structures of Sirenum Fossae extend across parts of the Eridania basin (Figs. 1, 6h and 8d), and other structures with similar east-west orientations cut across the northernmost part of this basin (Figs. 2 and 8c); the fractures that comprise the features of Sirenum Fossae are associated with a broader radial fracture network centered on Tharsis and believed to have been formed by the intrusion of dikes (Wilson and Head, 2002; Anderson et al., 2019). TES thermal inertia estimates indicate that parts of the Eridania basin are mantled by fines (Fig. 4b); nevertheless, exposures of relatively high thermal inertia materials are generally far more extensive than along much of the Ma'adim Vallis system itself, allowing for the improved characterization of local rock and bedrock mineralogy (Fig. 5). Large fields of flat-topped mesas and rounded knobs, consisting of partly-eroded materials of Late Noachian and Early Hesperian age that collectively have a superficial resemblance to chaotic terrain, are located within the lower elevations of several sub-basins including Ariadnes, Atlantis, and Gorgonum (e.g., Grant and Schultz, 1990; Howard and Moore, 2004; Capitan and Van De Wiel, 2011; Baker and Head, 2009, 2012; Wendt et al., 2013; Molina et al., 2014; Adeli et al., 2015; Michalski et al., 2017) (Figs. 1 and 6e). Parts of the Eridania basin are mantled by light-toned and Hesperian-aged Electris deposits (Fig. 6f), which have thicknesses of up to ~500 m and are distributed across a wide range of elevations (e.g., Grant and Schultz, 1990; Grant et al., 2010; Baker and Head, 2012; Molina et al., 2014). Channel systems of relatively limited extent and low areal density exist within the Eridania basin (e.g., Baker and Head, 2009; Howard and Moore, 2011; Adeli et al., 2015). Small cones and domes are

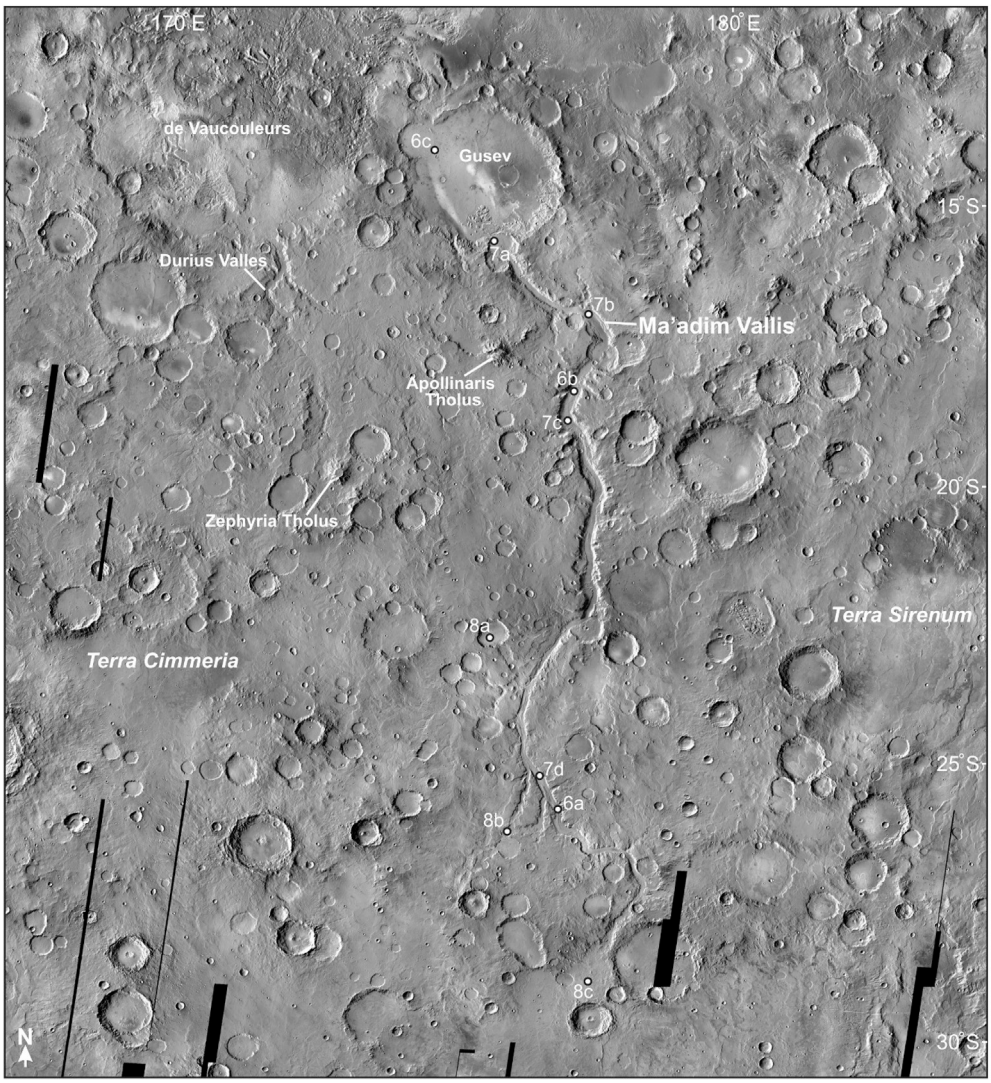

Fig. 3. Daytime Thermal Emission Imaging System (THEMIS) mosaic of the Ma'adim Vallis region. The locations of relevant areas depicted in Figs. 6–8 are given. Mosaic courtesy of Arizona State University. Equirectangular projection.

present here (e.g., Brož et al., 2015), and an irregularly-shaped crater complex exists at the intersection of Sirenum Fossae and orthogonal faults in Atlantis basin (e.g., Scott and Tanaka, 1986; Capitan and Van De Wiel, 2011) (Fig. 6g). Hydrous minerals such as chlorides, sulfates, and phyllosilicates are exposed at numerous locales of relatively limited extent within the Eridania basin and adjacent regions, confirming that some materials have interacted with water (e.g., Osterloo et al., 2008, 2010; Glotch et al., 2010; Davila et al., 2011; Ruesch et al., 2012; Carter et al., 2013; Wendt et al., 2013; Adeli et al., 2015; Pajola et al., 2016; Leask et al., 2017; Michalski et al., 2017) (Fig. 5c).

3. Past aqueous interpretations of Ma'adim Vallis

Formation of Ma'adim Vallis has been attributed to the past operation of aqueous processes involving one or more of the following: 1) surface runoff from adjacent intercrater plains (e.g., Schneeberger, 1989); 2) releases from one or more large highland lakes (e.g., Cabrol et al., 1998a; Irwin et al., 2002, 2004); 3) voluminous highland outflows of groundwater at sites of chaotic terrain or at the structures that comprise Sirenum Fossae (e.g., Landheim, 1995; Cabrol et al., 1998a b; Kuzmin et al., 2000; Gulick, 2001); and 4) basal sapping by groundwater (e.g., Sharp and Malin, 1975; Cabrol et al., 1998a; Gulick, 2001). Interpretations predominantly involving system development by large and sudden effusions of groundwater suggest categorization of Ma'adim Vallis as an outflow channel, whereas interpretations mainly involving other processes such as sapping or precipitation-driven runoff generally treat the system as a form of valley network (e.g., Parker, 2000; Gulick, 2001).

Aqueous interpretations of the Ma'adim Vallis channel system have previously led to hypotheses that water was once ponded within Gusev crater, within topographic basins located along the main channel of the system, and possibly within adjacent basins of the northern lowlands and southern highlands (e.g., Schneeberger, 1989; Goldspiel and Squyres, 1991; Cabrol et al., 1994, 1996, 1997, 1998a b, 1999; Grin and Cabrol, 1997; Cabrol and Grin, 2001; Carter et al., 2001; Irwin et al., 2002, 2004; Fassett and Head, 2008). Gusev crater deposits located near the mouth of Ma'adim Vallis have previously been hypothesized as the possible eroded remnants of a lacustrine delta or other sedimentary fill, as have deposits located near the mouths of several small valleys and channels incised into the inner rim of the crater (e.g., Schneeberger, 1989; Goldspiel and Squyres, 1991; Landheim et al., 1994; Grin and Cabrol, 1997; Cabrol et al., 1998b; Irwin et al., 2002, 2004). Deposits within the channels of Ma'adim Vallis, including some terrace and floor units, have previously been interpreted as possible sedimentary materials emplaced in fluvial or lacustrine environments (e.g., Cabrol et al., 1996, 1998b), though some of these units have also been interpreted as products of non-aqueous mechanisms such as aeolian processes (e.g., Kuzmin et al., 2000).

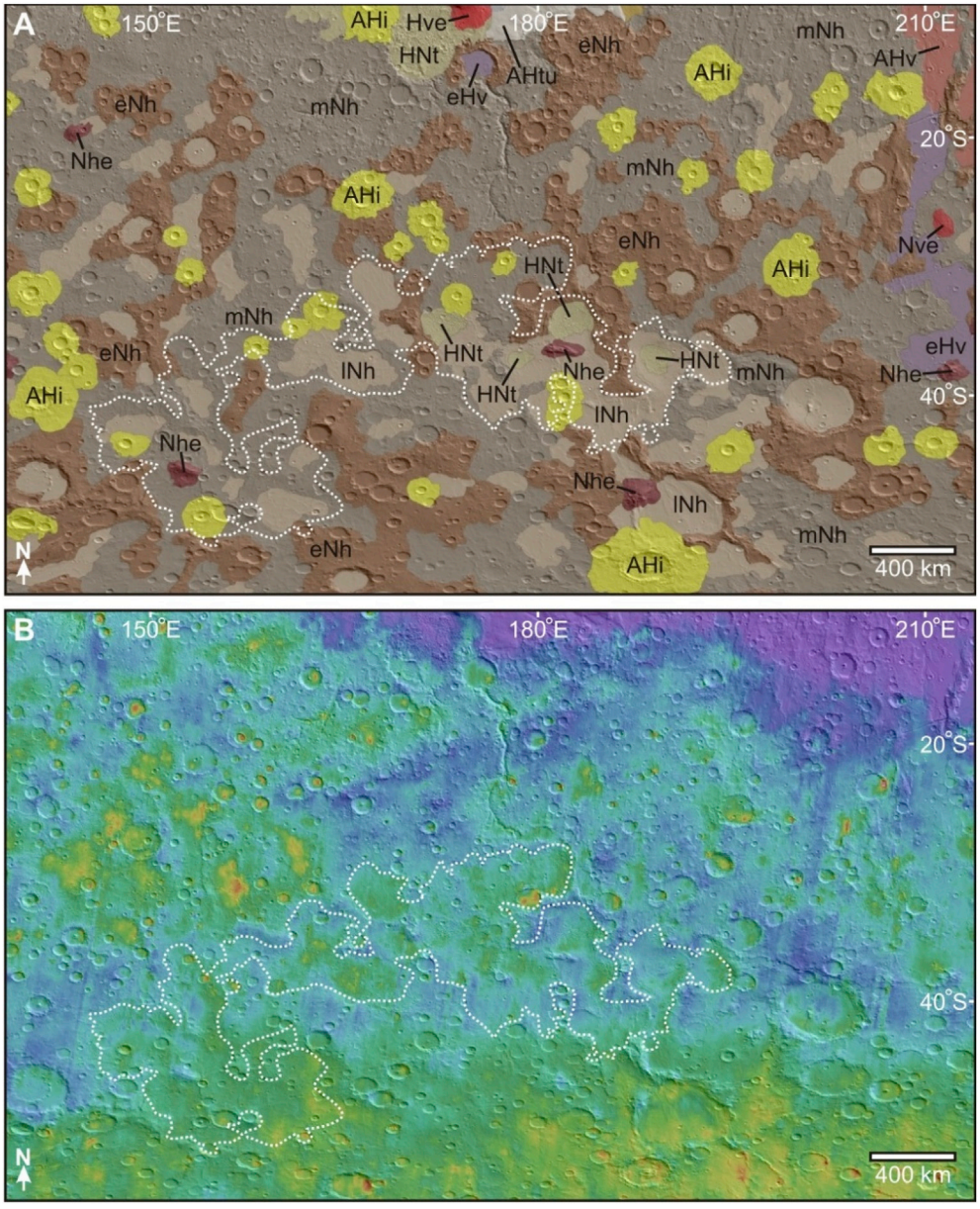

Fig. 4. Maps of surface geology (*A*) and thermal inertia (*B*) for the Ma'adim Vallis region and Eridania basin, overlain on hill-shaded MOLA topography. Gusev crater is at top center. Surface geology after Tanaka et al. (2014). Geological classes: *Nhe*: Noachian highland edifice unit; *Nve*: Noachian volcanic edifice unit; *eNh*: Early Noachian highland unit; *mNh*: Middle Noachian highland unit; *lNh*: Late Noachian highland unit; *HNt*: Hesperian and Noachian transition unit; *eHv*: Early Hesperian volcanic unit; *Hve*: Hesperian volcanic edifice unit; *AHtu*: Amazonian and Hesperian transition undivided unit; *AHi*: Amazonian and Hesperian impact unit (Tanaka et al., 2014). Thermal inertia (purple: ~40–90 tiu; dark blue: ~120–160 tiu; cyan: ~190–240; green: ~260–280 tiu; yellow: ~320–360 tiu; red: ~420–460 tiu) derived from measurements generated by the Thermal Emission Spectrometer (TES) (Christensen et al., 2001). The 1100 m contour of the main part of the previously hypothesized Eridania lake is given (dotted outline). Base maps generated using JMARS (Java Mission-planning and Analysis for Remote Sensing) software. MOLA topographic data after Smith et al. (2003). Equirectangular projection. (For interpretation of the references to colour in this figure legend, the reader is referred to the Web version of this article.)

Based in part on information collected *in situ* by the Spirit rover, clear examples of lacustrine sedimentary deposits are now recognized as missing in Gusev crater, and such deposits are widely assumed to have been buried by younger lava flows (e.g., Squyres et al., 2004). The hydrated Noachian-aged outcrops in the Columbia Hills are interpreted by some workers as possible products of evaporative precipitation or other processes operating in past lacustrine environments (e.g., Carter and Poulet, 2012; Ruff et al., 2014), though other interpretations have suggested alteration in highly localized hydrothermal environments that need not have been associated with such environments (e.g., Yen et al., 2008; Morris et al., 2010; Mittlefehldt et al., 2019).

Some researchers have previously interpreted Ma'adim Vallis as a product of multiple discrete episodes of flow that collectively occurred over a broad time frame extending from the Noachian to the Amazonian, with individual flow episodes separated by extended periods of geological time during which little or no system development took place (e.g., Grin and Cabrol, 1997; Cabrol et al., 1998a,b). The short and immature character of tributaries at Ma'adim Vallis has argued against sustained erosion by precipitation-related runoff, and has instead suggested the predominance of groundwater-related mechanisms such as sapping in channel formation (e.g., Cabrol et al., 1998a; Gulick, 2001; Aharonson et al., 2002). On Earth, sapping is ultimately driven by infiltration from the surface (e.g., Schumm et al., 1995), but the melting of ground ice as a result of hydrothermal processes or global swings in climate has been hypothesized as a process that may have driven the mobilization and release of groundwater in the Ma'adim Vallis region in such a manner as to accentuate the morphological signatures of groundwater processes over those of surface overflow (e.g., Cabrol et al., 1998a b). For example, some tributaries of Durius Valles (a valley network located immediately west of Ma'adim Vallis; see Figs. 2 and 3) originate in the vicinity of Zephyria Tholus, which has suggested to some workers the possible thermal influence of igneous plumbing systems on subsurface volatile stores in the region (e.g., Brakenridge, 1990; Cabrol et al., 1998a). Similarly, flow of groundwater from the structures that comprise Sirenum Fossae (Fig. 1) has been hypothesized for the highlands located south of Ma'adim Vallis and linked to the operation of ancient hydrothermal processes driven by Tharsis volcanism (e.g., Landheim, 1995; Cabrol et al., 1997; Cabrol et al., 1998a b).

In contrast with earlier interpretations of Ma'adim Vallis as a product of numerous separate phases of development that occurred over

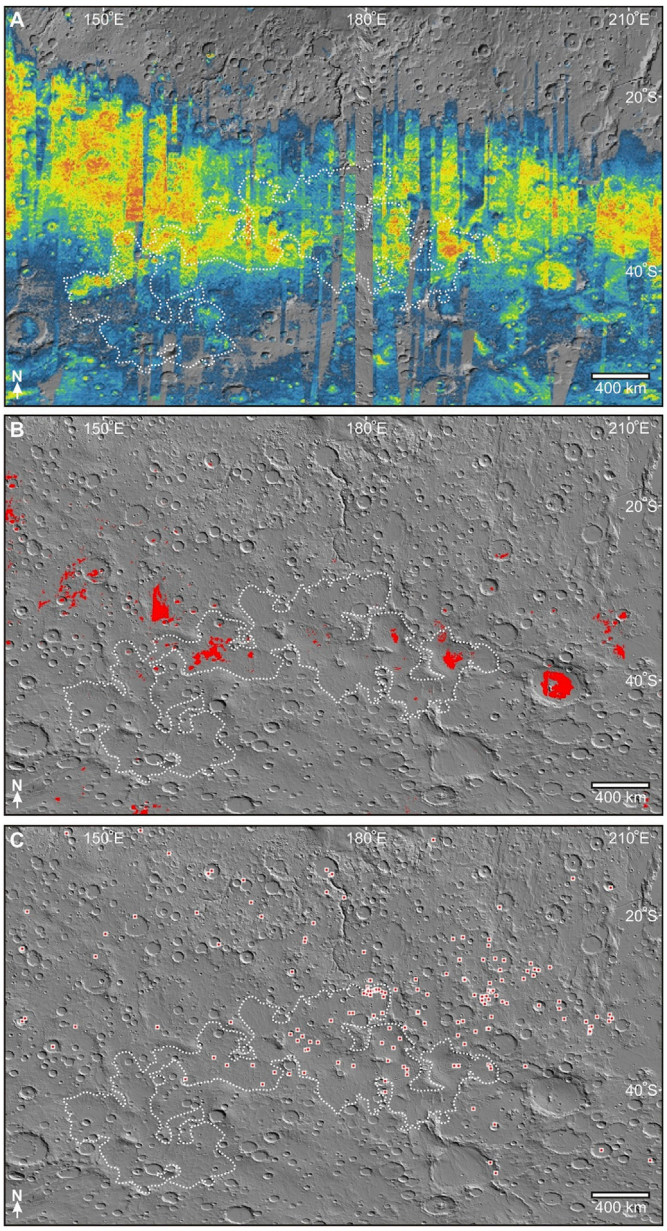

Fig. 5. OMEGA (Observatoire pour la Mineralogie, l'Eau, les Glaces et l'Activité) maps of pyroxene (*A*), high-olivine materials (*B*), and hydrous minerals (*C*) for the Ma'adim Vallis region and Eridania basin. Gusev crater is at top center. Pyroxene (blue = lower abundances; green = moderate abundances; yellow and red = higher abundances) and high-olivine maps (red = ~10% to >25% olivine) after Ody et al. (2012 ab, 2013). Sites of hydrous mineral exposures after Carter et al. (2013). Areas of relatively good surface exposure of coarser materials are highlighted by low-to-high pyroxene abundances in *A*; other areas in *A* are depicted in shades of gray and are generally mantled by relatively fine sediments dominated by anhydrous nanophase ferric oxides (Ody et al., 2012a,b) that were generated by processes that did not involve liquid water (Bibring et al., 2006). Mineral data are overlain on hillshaded MOLA topography. The 1100 m contour of the main part of the previously hypothesized Eridania lake is given (dotted outline). Base maps generated using JMARS software. MOLA topographic data after Smith et al. (2003). Equirectangular projection. (For interpretation of the references to colour in this figure legend, the reader is referred to the Web version of this article.)

extended periods of time, catastrophic formation of the system is hypothesized by some workers to have occurred as a result of the sudden partial drainage of a large and long-lived lake that is believed to have existed in the Eridania basin during much of the Late Noachian and possibly the Early Hesperian (mainly >3.8 Ga before present) (e.g., Irwin et al., 2002, 2004; Michalski et al., 2017) (Fig. 1). In this scenario, catastrophic floods from the lake are inferred to have occurred through two gaps in the northern divide of the topographic basin containing the lake (e.g., Irwin et al., 2002, 2004; Goudge et al., 2018) (Figs. 1 to 3). The elevations of these gaps have implied a maximum lake highstand of ~1,100 m to no more than ~1,250 m (Irwin et al., 2004) (Fig. 1). The total lake volume is predicted to have been at least as great as ~210,000 km^3, of which ~160,000 km^3 would have existed between the 950 m and 1100 m contours that define the water levels that could theoretically have contributed to northbound floodwaters (Irwin et al., 2002; Fassett and Head, 2008; Michalski et al., 2017). The initial pooling and long-term persistence of standing water within the Eridania basin is hypothesized to have been related to precipitation or, much more likely, groundwater upwelling (e.g., Irwin et al., 2004; Kleinhans, 2005; Fassett and Head, 2008; Baker and Head, 2012; see also Andrews-Hanna et al., 2007); channels present in the Eridania basin are widely interpreted as fluvial in origin (e.g., Grant and Schultz, 1990; Capitan and Van De Wiel, 2011; Howard and Moore, 2011), but the relatively small catchment area of the hypothesized lake and the low density of associated valley networks has suggested no more than a minor role for surface runoff in lake development (e.g., Fassett and Head, 2008; Baker and Head, 2009; Adeli et al., 2015). The large bowl-shaped depressions that comprise much the Eridania basin, in combination with the lower prevalence of channels within the Eridania basin at elevations below ~700 m, have suggested the long-term persistence of lake levels of at least 700 m during the main time frame of highland channel incision in the region (Irwin et al., 2002, 2004; Adeli et al., 2015; Michalski et al., 2017). Initial northward overflow of the lake is hypothesized to have possibly been triggered by an impact event, and is predicted to have initially led to the partial filling of a relatively small basin (the "Intermediate" basin) centered along the southernmost reaches of Ma'adim Vallis (Irwin et al., 2004) (Fig. 2). Peak aqueous discharges exceeding ~5×10^6 m^3/s have been estimated for development of Ma'adim Vallis, with overall water-to-sediment ratios of ~6:1 to 19:1 (Irwin et al., 2004). The occurrence of multiple separate flood events is considered possible but not essential (e.g., Irwin et al., 2004; Kleinhans, 2005).

Following development of the Ma'adim Vallis system by catastrophic floods, the remaining lake waters are expected to have been gradually lost as a result of evaporation and seepage within closed basins (e.g., Adeli et al., 2015). Only limited channel incision is generally believed to have taken place at Ma'adim Vallis and the Eridania basin following hypothesized flood events (e.g., Irwin et al., 2004), though water-related processes are interpreted by some workers to have operated in the Eridania basin well into the Amazonian (e.g., Capitan and Van De Wiel, 2011). With surface flow possibly restricted to localized runoff related to processes such as the melting of snow or ice deposits (e.g., Howard and Moore, 2011; Baker and Head, 2012), tributaries would have remained immature and the main Ma'adim Vallis channel left largely unmodified since the time frame of catastrophic flooding (Irwin et al., 2004).

Some plains units of the Eridania basin are interpreted as having been accumulated in fluvial or lacustrine environments (e.g., Capitan and Van De Wiel, 2011; Howard and Moore, 2011; Molina et al., 2014). Obvious shoreline deposits have not been identified within the Eridania basin (e.g., Irwin et al., 2004; Capitan and Van De Wiel, 2011; Adeli et al., 2015), but benches in Gorgonum basin have previously been interpreted as having formed in association with the development of an ancient ice-covered lake (Howard and Moore, 2004). Many of the plains that extensively mantle the Eridania basin are widely interpreted as volcanic in origin (e.g., Scott and Tanaka, 1986; Greeley and Guest, 1987; Irwin et al., 2004, 2013; Goudge et al., 2012; Baker and Head, 2009, 2012; Molina et al., 2014; Adeli et al., 2015; Brož et al., 2015; Michalski et al., 2017). An irregularly-shaped crater complex (Fig. 6g) is also interpreted as volcanic in origin (e.g., Scott and Tanaka, 1986; Capitan and Van De Wiel, 2011), and some Amazonian-aged plains units of local extent have properties suggestive of their emplacement as viscous lavas that were

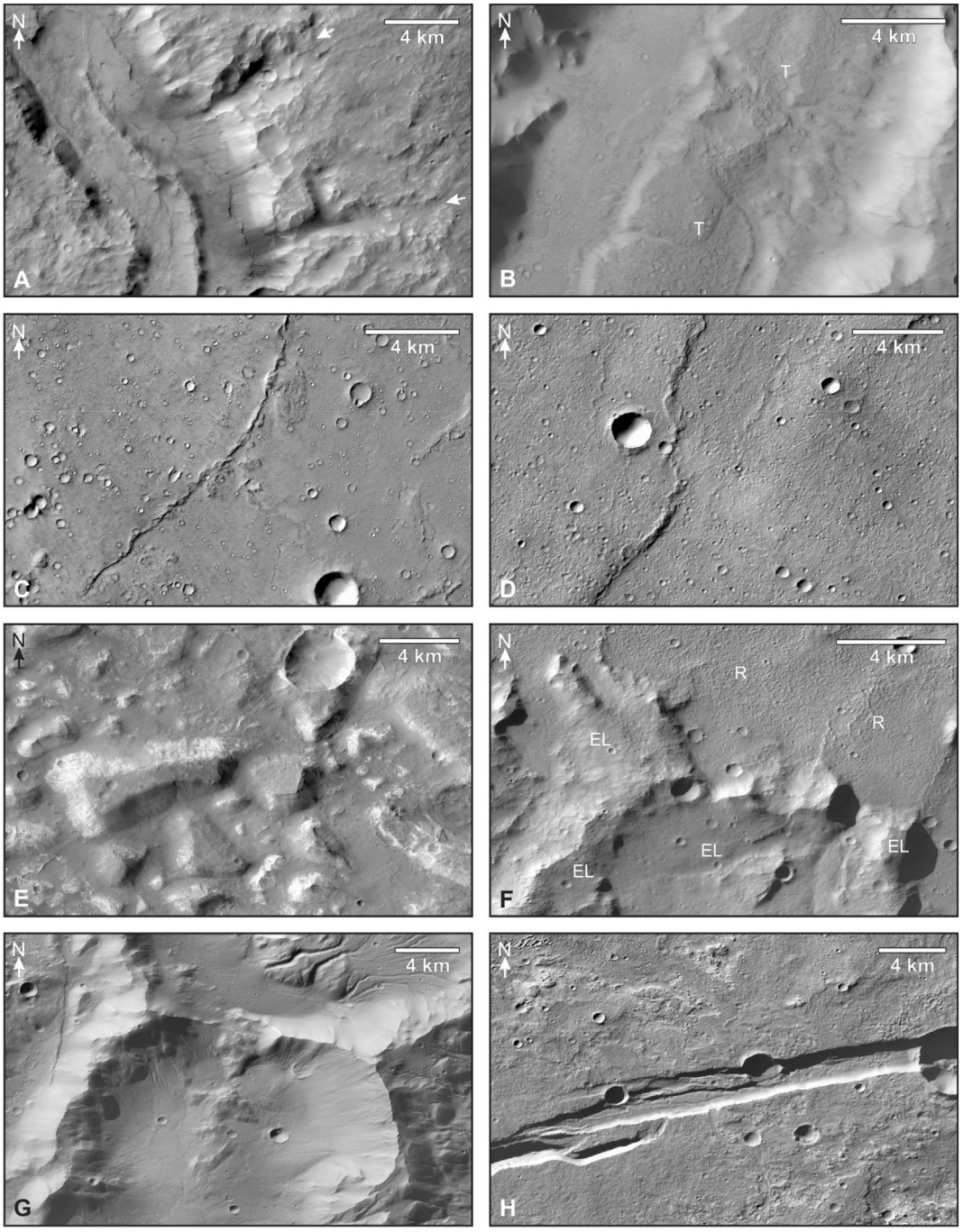

Fig. 6. Context Camera (CTX) images of selected landforms associated with Ma'adim Vallis and Eridania basin. *A*: Immature tributary valleys of Ma'adim Vallis (arrows). *B*: Terraces (*T*) of Ma'adim Vallis. *C*: Wrinkle-ridged plains of Gusev crater. *D*: Wrinkle-ridged plains typical of much of the Eridania basin. *E*: Flat-topped erosional residuals of Ariadnes Colles (Fig. 1). *F*: Electris deposits (*EL*) located south of Ariadnes Colles and immediately adjacent to ridged plains (*R*) (e.g., Grant et al., 2010). *G*: Part of a candidate volcanic complex located in the Eridania basin (e.g., Capitan and Van De Wiel, 2011). *H*: Graben-like structures of Sirenum Fossae. Wrinkle ridges develop within mare-style basalts as a result of processes related to subsidence (e.g., Schleicher et al., 2019), and are interpreted here as suggestive of the presence of analogous volcanic units. CTX images: *A*: P13_006168_1538_XN_26S183W; *B*: P02_001922_1595_XN_20S182W; *C*: G22_026804_1654_XN_14S185W; *D*: G18_025156_1473_XN_32S191W; *E*: P12_005799_1454_XN_34S187W; *F*: F01_036351_1403_XN_39S185W; *G*: B17_016413_1419_XI_38S173W; *H*: B21_017784_1425_XI_37S166W. Approximate figure centers: *A*: 25°47′S, 176°54′E; *B*: 18°15′S, 177°12′E; *C*: 14°02′S, 174°37′E; *D*: 32°21′S, 168°11′E; *E*: 34°49′S, 172°54′E; *F*: 37°46′S, 174°30′E; *G*: 37°45′S, 173°44′W; *H*: 36°30′S, 166°24′W. The locations of depicted areas are given in Fig. 1 and 3.

involved in development of some of the cones and domes of Eridania basin (Brož et al., 2015). Electris deposits are located at elevations both below and above the maximum level inferred for ancient lacustrine environments within the Eridania basin, and are generally interpreted as volcanic airfall deposits that were possibly redistributed by eolian processes (e.g., Grant and Schultz, 1990; Grant et al., 2010; Baker and Head, 2012; Molina et al., 2014).

The fields of flat-topped mesas and rounded knobs located at lower elevations within several impact basins of Eridania have been interpreted as possible products of aqueous outflows from the subsurface or, more likely, as deep basin deposits that accumulated in lacustrine environments (e.g., Baker and Head, 2012; Wendt et al., 2013; Adeli et al., 2015;

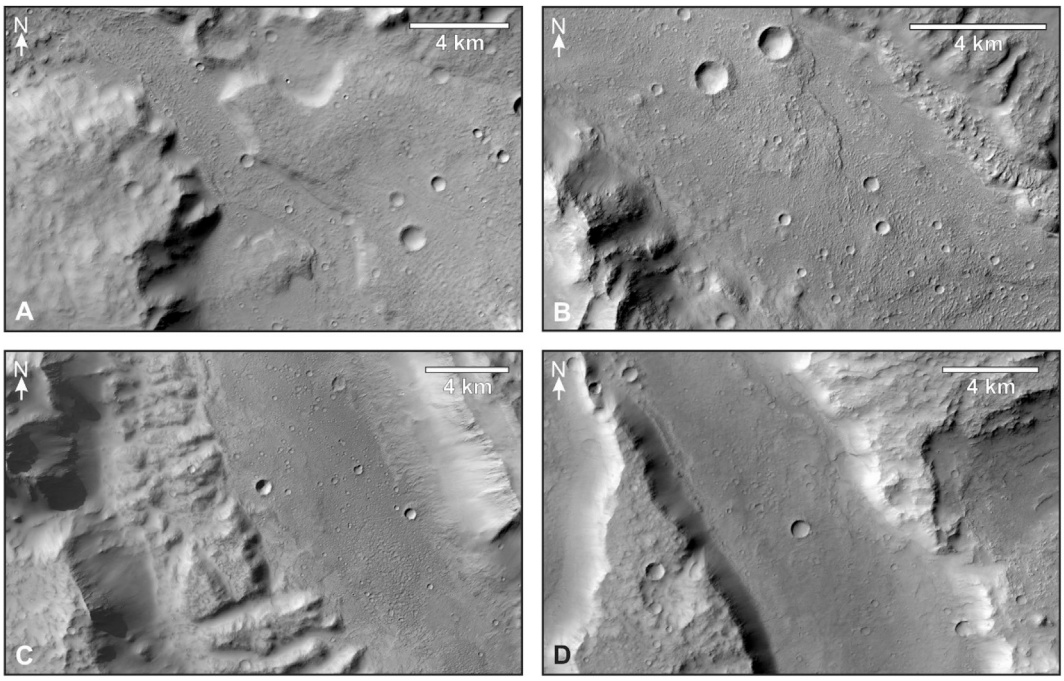

Fig. 7. The main Ma'adim Vallis channel is floored along numerous reaches by plains units interpreted as volcanic flows. CTX images: *A*: D20_034874_1653_XN_14S184W; *B*: F17_042496_1650_XI_15S183W; *C*: P22_009675_1591_XI_20S182W; *D*: J03_045951_1554_XN_24S183W. Approximate figure centers: *A*: 15°41′S, 175°44′E; *B*: 16°57′S, 177°21′E; *C*: 18°52′S, 177°2′E; *D*: 25°15′S, 176°31′E. The locations of depicted areas are given in Fig. 3.

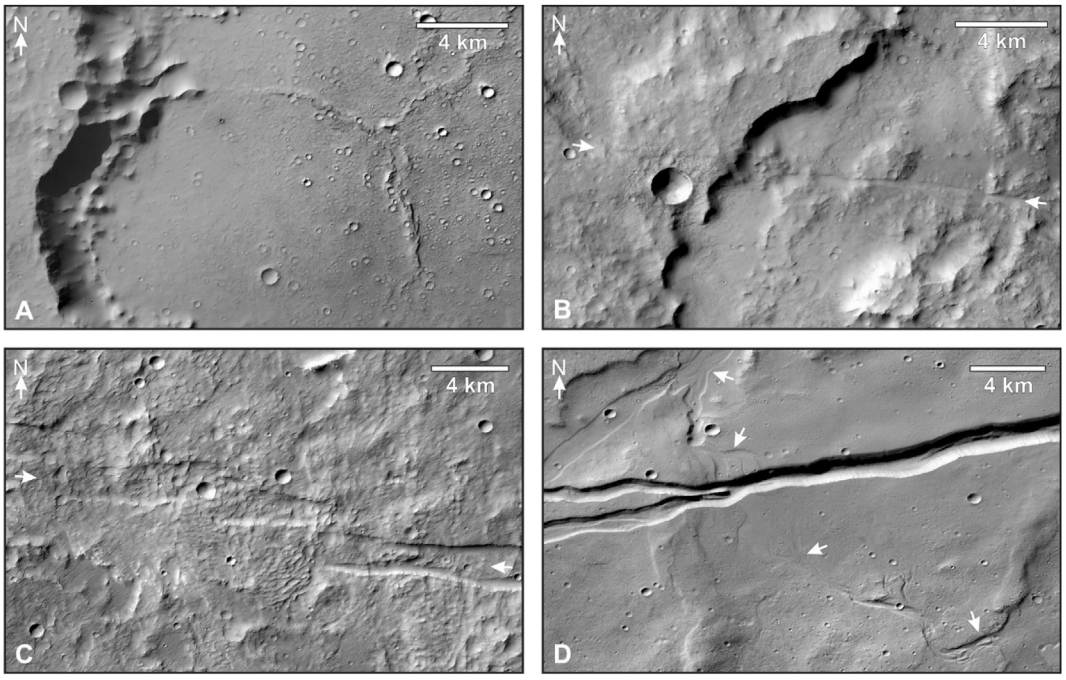

Fig. 8. *A*: Ridged plains associated with impact craters located within the Intermediate basin. *B*: An east-west oriented structure (between arrows) that crosses the Intermediate basin. *C*: En echelon graben-like structures oriented east-west (between arrows) and crossing the Eridania basin near the head of Ma'adim Vallis. *D*: An example of Sirenum Fossae structures associated with channels (e.g., at arrows). CTX images: *A*: B19_017099_1571_XN_22S184W; *B*: B17_016110_1547_XN_25S184W; *C*: B17_016466_1513_XI_28S182W; *D*: B18_016611_1393_XN_40S179W. Approximate figure centers: *A*: 22°44′S, 175°34′E; *B*: 26°15′S, 175°55′E; *C*: 28°54′S, 177°19′E; *D*: 39°25′S, 179°51′E. The locations of depicted areas are given in Fig. 1 and 3.

Michalski et al., 2017, 2018). Partly mantled by younger Hesperian-aged and relatively unaltered volcanic deposits, these units are in places associated with exposures of clay-, carbonate-, and possible sulfate-bearing materials (e.g., Wendt et al., 2013; Adeli et al., 2015; Michalski et al., 2017, 2018) that have suggested the presence of deep-water hydrothermal deposits of possible astrobiological interest (e.g., Michalski et al., 2017, 2018). Many of the chlorides, sulfates, and phyllosilicates exposed within and near the Eridania basin are hypothesized to have been formed as a result of local groundwater upwelling, surface runoff, and/or ponding (e.g., Ruesch et al., 2012; Osterloo et al.,

2010; Adeli et al., 2015; Pajola et al., 2016).

4. Problems with aqueous interpretations of Ma'adim Vallis

Though some landforms and geological units at Ma'adim Vallis have previously been interpreted as having been formed by aqueous processes (e.g., Schneeberger, 1989; Goldspiel and Squyres, 1991; Landheim et al., 1994; Grin and Cabrol, 1997; Cabrol et al., 1998b; Irwin et al., 2002, 2004), obvious examples of fluvial, diluvial, or lacustrine sedimentary deposits have proven difficult to identify. Impact and aeolian features are abundant at this system (e.g., Cabrol et al., 1998a; Kuzmin et al., 2000), and many features associated with channel reaches and terminal basins have general appearances and properties most consistent with volcanic origins (e.g., Grant et al., 2004; Golombek et al., 2005; Greeley et al., 2005) (Figs. 6cdf and 7). Much of Ma'adim Vallis is blanketed by anhydrous fines that partly obscure the mineralogy of underlying materials (Figs. 4 and 5), but the mouth of the system at Gusev crater has been investigated *in situ* and is known to be substantially mantled by mineralogically pristine volcanic flows of mafic and ultramafic composition and of Hesperian age (e.g., Gellert et al., 2004; Morris et al., 2004; Squyres et al., 2004; Greeley et al., 2005; Arvidson et al., 2006).

Martian igneous units exposed to aqueous conditions should become altered within years to millennia, depending on factors such as water abundances, water pH levels, and local temperatures (e.g., Oze and Sharma, 2007; Hausrath et al., 2008). Where exposure is good, electromagnetic radiation reflected by such altered units will normally display spectral features indicative of the presence of hydrated minerals (e.g., Noe Dobrea et al., 2003; Pommerol and Schmitt, 2008; Leverington and Moon, 2012; Weitz et al., 2014; Wang et al., 2018; see also, e.g., Baker et al., 2000), and the pristine character of the Hesperian-aged volcanic flows of Gusev crater is not expected of former lacustrine environments (e.g., Squyres et al., 2004; Haskin et al., 2005; Morris et al., 2006; Mittlefehldt et al., 2019). Hydrated minerals are locally present in Gusev crater at sites associated with the Noachian-aged Columbia Hills (e.g., Ming et al., 2006; Squyres et al., 2006, 2008; Morris et al., 2006), but these minerals apparently formed in low water-to-rock ratios that do not require development in lacustrine environments (e.g., Yet et al., 2008; Morris et al., 2010; Mittlefehldt et al., 2019). Assumptions that lacustrine sedimentary deposits of Gusev crater must exist beneath the younger Hesperian-aged volcanic flows (e.g., Squyres et al., 2004) are based mainly on presumed aqueous origins for the channels of Ma'adim Vallis rather than on the properties of local units or landforms.

Clear geomorphological evidence for the past existence of one or more large lakes in the Eridania basin over geological timescales is lacking. Some Eridania units are hypothesized to have been deposited in lacustrine environments, but these interpretations are equivocal. For example, the colles and chaos deposits associated with the lowest elevations of some basins are considered by some workers to be candidates for deep-water deposits (e.g., Michalski et al., 2017, 2018), but the true origins of these deposits remain uncertain and their basic properties do not appear to require development in large water bodies. The past existence of a lake over geological timescales should have resulted in the accumulation of far more extensive sedimentary mantles across the Eridania basin, and the gradual loss of lake waters should have resulted in the generation of a series of progressively lower shoreline and nearshore sedimentary deposits. Yet, no shoreline features have been identified within the Eridania basin (e.g., strandline deposits, spits, or offshore bars), including at the ~1100 m elevation believed to have characterized the maximum level of lake waters (e.g., Irwin et al., 2004; Capitan and Van De Wiel, 2011; Adeli et al., 2015), and there is no obvious evidence that extensive sedimentary mantles of lacustrine origin have ever existed here. This absence could conceivably be related to an overestimation of the length of time over which the region was subjected to lacustrine conditions. Erosion or burial of ancient sedimentary units is also possible, but should these processes have had the capacity to eliminate exposure of all clear examples of aqueous sedimentary deposits within a basin that is roughly two thousand kilometers across?

The mineralogical properties of the Eridania basin are also not consistent with the past existence of an enormous and long-lived lake that suddenly released a proportion of its volume in catastrophic floods and then lost its substantial remaining waters through evaporation or sublimation within closed highland basins. Exposures of hydrous minerals are widespread in the Eridania region (e.g., Pajola et al., 2016; Michalski et al., 2017) (Fig. 5c), but they are in many cases of modest geographic extent (e.g., Osterloo et al., 2008, 2010), are typically separated by considerable expanses of little altered materials (e.g., Carter et al., 2013), and are distributed at elevations and in locales that are not consistently associated with hypothesized paleolake basins (e.g., Adeli et al., 2015). Extensive outcrops of the full range of evaporite minerals expected of the past sites of large lakes that were gradually lost through evaporation or sublimation (e.g., Leverington, 2011; see also e.g., Hills, 1984; Krijgsman et al., 1999; Zavialov et al., 2003) are missing within the Eridania basin (e.g., Adeli et al., 2015). The limited exposures of chloride minerals within and near the Eridania basin need not have been generated within lacustrine environments, and instead could have been derived from local magmas (Leask et al., 2017). Mechanisms similarly exist for formation of local sulfate minerals through volcanic processes, without the need to hypothesize the past existence of large water bodies and requisite high atmospheric pressures (e.g., Niles et al., 2017). Wrinkle ridges form in the mafic and related volcanic units of expansive volcanic plains and the interiors of impact basins (e.g., Wilhelms, 1987; Watters, 1988; Watters and Johnson, 2010; Watters and Nimmo, 2010; Schleicher et al., 2019), and the ridged plains units of the Eridania basin are correspondingly interpreted here as very likely of volcanic origin. Consistent with such an interpretation, the plains of Eridania are largely spectrally bland apart from signatures related to minerals such as pyroxenes (Baker and Head, 2012) (Fig. 5a). Large exposures of pristine olivine-rich materials exist both inside and outside of Eridania basin (e.g., Ody et al., 2011, 2012a b, 2013; Riu et al., 2019) (Fig. 5b), and units of this type should have been especially susceptible to alteration in younger aqueous environments of all kinds (e.g., Leverington, 2011). Where Hesperian-aged or younger units exist within the Eridania basin, it is conceivable that expected areas of hydration and lacustrine deposition are simply buried, but as at Gusev crater, this is arguably not an economical interpretation of landforms and geological units that can be explained as products of simpler and more realistic processes.

From a global perspective, the persistence of extensive and pristine olivine-rich units of Noachian age at numerous locales on Mars (e.g., Hoefen et al., 2003; Rogers et al., 2005; Bibring et al., 2006; Koeppen and Hamilton, 2008; Ody et al., 2012b; Wilson and Mustard, 2013; Amador et al., 2018; Riu et al., 2019; Mandon et al., 2020) is not compatible with the younger existence of wet surface conditions on this planet across large areas over geological time scales (Leverington, 2009, 2011, 2019a b; Leone, 2014, 2018, 2020), including the long-term existence of an enormous lake in the Eridania basin at the end of the Noachian Period and the beginning of the Hesperian Period. The absence on Mars of expected correlations between hydrated minerals and both highland channel networks and outflow channels (e.g., Bibring et al., 2006; Mangold et al., 2008; Carter et al., 2013; Wilson and Mustard, 2013; Ehlmann, 2014; Kaufman et al., 2019; Leverington, 2019b) contradicts hypothesized aqueous origins for these features and reinforces the perspective that cold and dry surface conditions have very likely dominated over the history of the planet (e.g., Leverington, 2009, 2011, 2019a b; Leone, 2014, 2018, 2020). The expected mineralogical and geomorphological signatures of ancient lowland oceans and highland lakes are also yet to be identified on Mars (e.g., Malin and Edgett, 1999; Ghatan and Zimbelman, 2006; Fairén et al., 2011; Leverington, 2011; Mouginot et al., 2012; Pretlow, 2013; Leone, 2014, 2020; Goudge et al., 2015; Pan et al., 2017; Sholes et al., 2019), in opposition to past inferences of the existence of such water bodies and associated periods of warmer temperatures and high atmospheric pressures (e.g., Leverington, 2009, 2011, 2019a b; Leone, 2014, 2018, 2020).

5. A volcanic interpretation of Ma'adim Vallis

The properties of Ma'adim Vallis are most consistent with dry volcanic origins involving effusions of low-viscosity flood lavas from multiple highland sources mainly during the Noachian and Hesperian. As is typical of flood lavas emplaced on bodies such as the Moon, Mercury, and Venus (e.g., Wilhelms, 1987; Byrne et al., 2013; Ivanov and Head, 2013; Zhang et al., 2016), most of these volcanic sources are expected to have been buried by the plains units with which they are associated. Martian highland terrains were extensively resurfaced by low-viscosity lavas in the Noachian and Hesperian (e.g., Goldspiel and Squyres, 1991), and mare-style ridged volcanic plains correspondingly extend across highland regions adjacent to most of the Ma'adim Vallis system, including areas within the Intermediate basin and the Eridania basin.

Though volcanic plains of the Ma'adim Vallis region could conceivably be mere volcanic mantles of landscapes associated with an otherwise aqueously-formed channel system, the absence of clear evidence for the past development of local channels by aqueous processes and the direct association of volcanic plains with component channels suggests the need to consider channel origins involving these lavas. Accumulation of low-viscosity lavas near the mouth of Ma'adim Vallis is indicated by the presence of ridged plains and by the petrological characteristics of related units examined by the Spirit rover (e.g., Grant et al., 2004; Golombek et al., 2005; Greeley et al., 2005; Chevrel et al., 2014). The flows that mantle the interior of Gusev crater have not been linked to particular volcanic vents and are interpreted by some workers as having possibly been erupted from local sources situated in or near the crater itself (e.g., Grant et al., 2004), but these flows could alternatively have been emplaced inside Gusev crater from more southerly sources. The geochemical properties of the Adirondack class lavas, which are especially abundant among the materials exposed at the surface of Gusev crater, suggest liquidus viscosities at least as low as 0.5 Pa s (Chevrel et al., 2014). Martian lavas with such viscosities can rise through igneous plumbing systems much faster than the much more viscous lavas typical of modern Earth (Chevrel et al., 2014) and have a substantial capacity for deep incision into bedrock substrates if erupted at sufficiently high rates and with high total volumes (e.g., Jaeger et al., 2010; Hurwitz et al., 2010; Dundas and Keszthelyi, 2014; Hopper and Leverington, 2014; Cataldo et al., 2015; Baumgartner et al., 2017; Leverington, 2018, 2019a b; Dundas et al., 2019; Vetere et al., 2019; Gasparri et al., 2020). Large magmatic plumbing systems that have roots within the upper mantle appear to be especially well suited for driving voluminous eruptions of the kind that formed large volcanic channel systems on Mars (Leverington, 2011, 2019a).

The floor of the Eridania basin is widely mantled by ridged plains that have characteristics similar to those of lunar flood lavas (e.g., Scott and Tanaka, 1986; Greeley and Guest, 1987; Irwin et al., 2004, 2013; Baker and Head, 2009; Goudge et al., 2012; Baker and Head, 2009, 2012; Molina et al., 2014; Tanaka et al., 2014; Adeli et al., 2015; Brož et al., 2015; Pajola et al., 2016; Michalski et al., 2017), and some of the lavas involved in development of Ma'adim Vallis are hypothesized to have flowed northward from this basin. Though most of the volcanic sources involved in emplacement of these plains units are expected to be buried, candidate examples of exposed volcanic sources include the graben-like structures of Sirenum Fossae and other Tharsis-radial structural features in the region, some of which are located near the head of Ma'adim Vallis (Fig. 2) and some of which are associated with channels (Fig. 8d). Such Tharsis-radial structural features were sources of fluid effusions from the subsurface along Mangala Fossa and some segments of Sirenum Fossae (e.g., Cabrol et al., 1998a; Leverington, 2007), and on this basis the formation of Ma'adim Vallis has previously been interpreted as potentially analogous to formation of the larger Mangala Valles outflow system to the east (e.g., Cabrol et al., 1998a); the Mangala Valles system is recognized by some workers as a product of the effusion of flood lavas from Mangala Fossa (Leverington, 2007, 2011; Leone, 2017). Other landforms of potential relevance to the volcanic development of Eridania basin units include candidate volcanic complexes, some of which have close spatial associations with the structures that comprise Sirenum Fossae (e.g., Capitan and Van De Wiel, 2011) (Fig. 6g). Small cones, domes, and craters of the Eridania basin also show volcanic affinities (Brož et al., 2015), and the Electris deposits are generally interpreted as volcanic airfall deposits (e.g., Grant and Schultz, 1990; Grant et al., 2010; Baker and Head, 2012; Molina et al., 2014).

If the colles and chaos landforms of the Eridania basin are analogous in origin to the chaotic terrain that characterizes some Martian outflow channels, then igneous processes related to magma intrusion, effusion, and drainback are similarly implicated in the disruption of associated units (e.g., Leverington, 2011, 2019a), along with secondary mechanisms such as mass wasting and aeolian deflation. In the eastern parts of the Eridania region, weakly-layered lava and ash deposits that have been disrupted to form chaotic terrain (Michalski et al., 2017) have appearances consistent with the past operation of such processes. In contrast, the materials that comprise the colles and chaos of the western and central parts of the Eridania basin do not show prominent layering and in places are crossed by systems of veins, and the origins of associated landforms are less clearly aligned with those of chaotic terrain typical of the outflow channels (Michalski et al., 2017). These western and central regions of colles and chaos could conceivably have nevertheless formed as a result of terrain disruption by igneous processes, but alternatively could represent erosional residuals of volcanic or aeolian units that accumulated in predominantly dry environments at basin centers.

Parts of the Intermediate basin of Ma'adim Vallis are characterized by the presence of ridged plains (Fig. 8a) of a character very similar to that of the plains at Gusev crater and within the Eridania basin. As with other highland areas including those located in the Ma'adim Vallis region (e.g., Leverington and Maxwell, 2004; Leverington, 2005, 2006), this suggests emplacement here of low-viscosity lava flows from sources both inside and outside of impact craters. The channels that extend from some of these craters (e.g., Capitan and Van De Wiel, 2011) suggest incision by associated lavas during periods of overflow, and thus formation of the Ma'adim Vallis system is expected to have been partly a product of the effusion of these lavas. Eruption of magmas within impact craters is not unexpected, as Martian impact craters are in numerous cases partly filled by ridged volcanic units that in many cases appear to require local sources (e.g., Leverington and Maxwell, 2004; Leverington, 2005, 2006). Obvious volcanic source features such as pits and volcanic cones can be associated with impact craters on rocky planets of the inner solar system (e.g., Gillis-Davis et al., 2009; Thomas et al., 2014), and candidate mechanisms for eruption within Martian craters include processes such as impact-induced decompression melting (Edwards et al., 2014).

Close spatial relationships between volcanic features and highland channels are not restricted to the Ma'adim Vallis system in this region. For example, channels extend from Zephyria Tholus (e.g., Brakenridge, 1990; Cabrol et al., 1998a), and highland channel networks located to the east in Memnonia are widely associated with low-viscosity lava flows likely to have had the capacity to incise these networks (Leverington and Maxwell, 2004). More broadly, volcanic associations with both highland channel networks and outflow channels are widespread on Mars (e.g., Plescia, 1990; Keszthelyi et al., 2000, 2004; Leverington, 2004, 2005, 2006, 2009, 2011, 2014, 2018a, 2019a b; Chapman et al., 2010a b; Jaeger et al., 2010; Hopper and Leverington, 2014; Dundas and Keszthelyi, 2014; Leone, 2014, 2017, 2020; Baumgartner et al., 2017; Hamilton et al., 2018; Dundas et al., 2019; Gasparri et al., 2020). Unlike past aqueous interpretations, the volcanic hypothesis for formation of Ma'adim Vallis is consistent with the overall geomorphological and mineralogical characteristics of the surface of Mars, and does not require the existence of unexpectedly large reservoirs of near-surface volatiles or thick ancient atmospheres (e.g., Leverington, 2011). Globally, the spatial distribution of Martian channels of all kinds lacks expected correlations with the distributions of hydrated minerals (e.g., Bibring et al., 2006; Mangold et al., 2008; Carter et al., 2013; Wilson and Mustard, 2013; Ehlmann, 2014; Kaufman et al., 2019), bringing into question past

interpretations of these channels as having been formed by aqueous overflow that drove incision into geological units purported to have hosted groundwater and ground ice over geological timescales (e.g., Leverington, 2011, 2019a b; Leone, 2014, 2018, 2020).

Some aqueous interpretations of the Ma'adim Vallis system have been partly based upon explicit and implicit assumptions that lava plains within closed basins should not have bowl-shaped surfaces (e.g., Irwin et al., 2002, 2004) and should mark the highest levels attained by these flows. However, lava levels within topographic basins can indeed decrease during or after eruptions as a result of processes such lava degassing, lava contraction during solidification, and late-stage lava drainback into magmatic plumbing systems (e.g., Leverington, 2009; 2011, 2019a b). For example, Aromatum Chaos, the ~30 × 90 km head depression of Martian channel Ravi Vallis, is interpreted by Leverington (2019a) as the volcanic source of this outflow system and has a floor that is as much as ~1.5 km beneath the adjacent channel floor (Carr, 2012). Also, the modern elevations of lava infill need not be uniform across individual basins, with the flood lavas that occupy the interiors of large impact basins on Mars and other bodies of the inner solar system typically varying in elevation by hundreds of meters to kilometers, in some cases defining basin surfaces with distinct bowl shapes (e.g., Kaula et al., 1973; Wieczorek and Phillips, 1999; Thomson and Head, 2001; Oberst et al., 2010; Ivanov et al., 2012). For example, vertical variations in the bowl-shaped and lava-mantled surfaces of Martian basins Isidis and Utopia are roughly as great as ~370 m and 1 km, respectively (Smith et al., 2003). Loading of the various parts of Eridania basin by wrinkle-ridged lava flows is hypothesized by some workers to have contributed to development of the bowl shapes of component impact basins (Baker and Head, 2009).

6. Development of Ma'adim Vallis channels by flood lavas

Though formation of large volcanic channels by low-viscosity lavas is exotic by modern terrestrial standards, hundreds of ancient channel systems of volcanic origin are preserved on the Moon, Venus, Mercury, and Earth (e.g., Greeley, 1971; Gornitz, 1973; Schultz, 1976; Wilhelms, 1987; Baker et al., 1992, 1997; Head et al., 1992, 2011; Williams et al., 2001, 2011; Byrne et al., 2013; Hurwitz et al., 2013a b; Komatsu et al., 1993; Komatsu, 2007; Roberts and Gregg, 2019) (Fig. 9). Many of these analog systems formed as outflow channels that commence at distinct topographic lows that mark sites of voluminous lava effusion, but others developed as low-order branching networks that formed during emplacement of lavas from multiple sources in complex terrain (e.g., Wilhelms, 1987; Baker et al., 1992, 1997; Komatsu et al., 1993; Leverington, 2011, 2014; Hurwitz et al., 2013a b). Except on Venus, where early landscapes have been entirely lost as a result of erosion and extensive resurfacing, preserved volcanic analog systems were formed primarily in the first 1–2 Ga of solar system history, a time frame characterized by higher interior temperatures and greater associated propensities to form large volumes of low-viscosity lavas in geological environments such as plumes (e.g., Leverington, 2011, 2014, 2019a). This early time frame overlaps with both the Noachian and Hesperian periods of Mars (e.g., Hartmann, 2005), and thus coincides with the main interval of development of the Ma'adim Vallis system and numerous

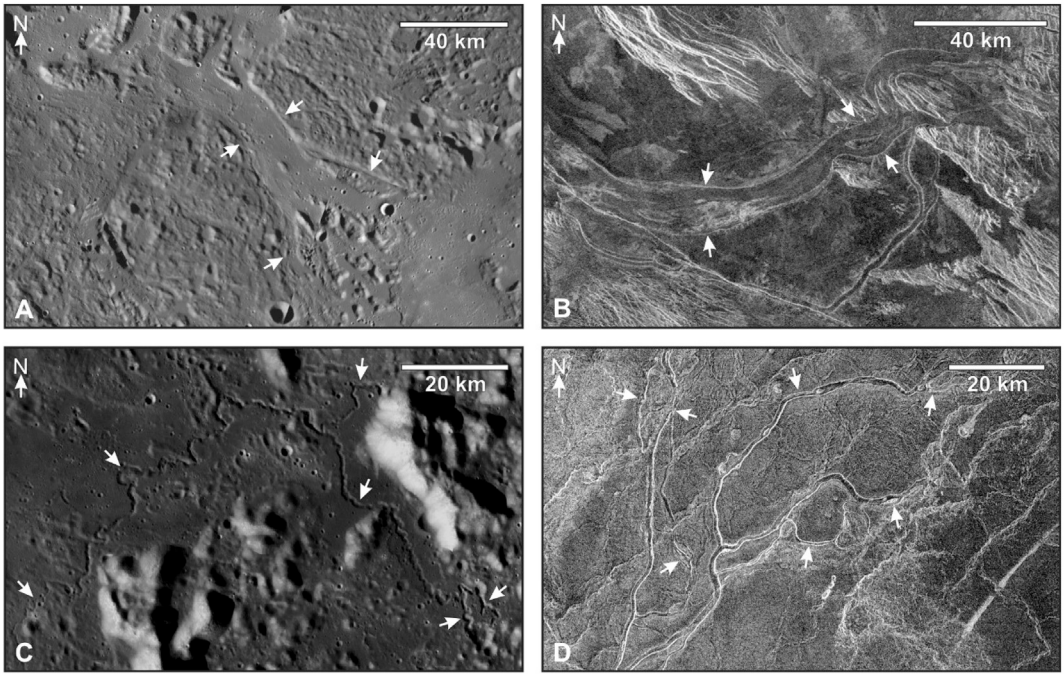

Fig. 9. Ancient volcanic channels of a wide variety of sizes and complexities are preserved at the surfaces of large rocky bodies of the inner solar system (e.g., Leverington, 2014). *A*: Angkor Vallis is a relatively short channel that connects two large Mercurian basins that are mantled by mare-style ridged plains (e.g., Head et al., 2011; Byrne et al., 2013; Hurwitz et al., 2013b). *B*: With a length of more than 1000 km and a major igneous source region marked by chaotic terrain, Kallistos Vallis is among the largest volcanic channels on Venus and has characteristics similar to those that typify the Martian outflow channels (e.g., Baker et al., 1992, 1997; Hopper and Leverington, 2014). This system attests to the capacity of low-viscosity lavas to form channel systems with sizes similar to that of Ma'adim Vallis. Unlike Kallistos Vallis, Ma'adim Vallis is interpreted here to have formed as a result of voluminous effusions from numerous volcanic sources that emplaced extensive ridged plains, rather than from a major source marked only by chaotic terrain. *C*: The lunar Rimae Plato group consists of several channel systems including this low-order network (arrows) that originates among highlands adjacent to Mare Imbrium (e.g., Leverington, 2006; Hurwitz et al., 2013a). *D*: Ganga Valles is a complex network of sinuous Venusian channels (arrows) located west of Disani Corona (e.g., Komatsu et al., 1993; Campbell and Clark, 2006; Leverington, 2011). Branching channel networks such as those of the Moon and Venus confirm that low-order volcanic systems of some complexity can develop where multiple igneous sources have driven channel development. Image sources: *A*: Mercury MESSENGER (MErcury Surface, Space ENvironment, GEochemistry, and Ranging) MDIS (Mercury Dual Imaging System) Global Basemap. *B* and *D*: Magellan FMAP (full-resolution radar map) left-look radar mosaic. *C*: LRO (Lunar Reconnaissance Orbiter) WAC (Wide Angle Camera) Mosaic. Approximate figure centers: *A*:57°54′N, 113°12′E; *B*: 51°12′S, 22°32′E; *C*: 49°30′N, 2°6′W; *D*: 5°N, 53°8′E.

other large channel systems on Mars. Though opposing aqueous interpretations have dominated for decades (e.g., Baker and Milton, 1974; Baker and Kochel, 1978a b; Carr, 1979, 1996; Baker et al., 1991; Carr and Head, 2015; Lepotre et al., 2016; Larsen and Lamb, 2016; Head et al., 2018), the properties of the Martian outflow channels are consistent with formation by dry volcanic processes (e.g., Schonfeld, 1979; Leverington, 2004, 2007, 2009, 2011, 2014, 2018, 2019a b; Hopper and Leverington, 2014; Leone, 2014, 2017, 2018, 2020; Baumgartner et al., 2015, 2017), and some workers contend that evidence for analogous development of highland channel systems by effusion of flood lavas is also widespread on Mars (Leverington and Maxwell, 2004; Leverington, 2005, 2006; 2011; Leone, 2014, 2020; Gasparri et al., 2020).

Low-viscosity lavas erupted at high rates of effusion and large total volumes possess the capacity for erosional development of immense volcanic channels through both mechanical and thermal processes (e.g., Peterson and Swanson, 1974; Hulme and Fielder, 1977; Hulme, 1982; Huppert et al., 1984; Lesher and Campbell, 1993; Greeley et al., 1998; Williams et al., 2000, 2011; Barnes, 2006; Houlé et al., 2008, 2012; Jaeger et al., 2010; Hurwitz et al., 2012, 2013b; Stockstill-Cahill et al., 2012; Gole et al., 2013; Dundas and Keszthelyi, 2014; Hopper and Leverington, 2014; Leverington, 2014, 2018, 2019a b; Baumgartner et al., 2015, 2017; Cataldo et al., 2015; Staude et al., 2016, 2017; Lesher, 2017; Vetere et al., 2019; Gasparri et al., 2020). The minimum viscosities of ancient flood lavas involved in landscape resurfacing or channel development in the inner solar system (including on the Moon, Venus, Mercury, and Earth) were at least as low as ~0.1–10 Pa s (e.g., Murase and McBirney, 1970, 1973; Weill et al., 1971; Kargel et al., 1993; Williams et al., 2001, 2011; Stockstill-Cahill et al., 2012; Byrne et al., 2013; Leverington, 2014; Vetere et al., 2017; Lesher, 2017; Peplowski and Stockstill-Cahill, 2019), and thus were up to several orders of magnitude lower than the ~50–5000 Pa s typical of the least viscous silicate lavas erupted on Earth today (e.g., Shaw et al., 1968; Murase and McBirney, 1973; Self et al., 1997). The Adirondack class lavas near the mouth of Ma'adim Vallis have geochemical properties that suggest liquidus viscosities of only ~0.5 Pa s (Chevrel et al., 2014).

Though much remains to be learned with regard to the precise manner in which large volcanic channel systems are formed by low-viscosity lavas (e.g., Dundas and Keszthelyi, 2014; Cataldo et al., 2015; Baumgartner et al., 2017), the past study of both volcanic and fluvial systems has led to progress in the use of quantitative methods for estimation of flow conditions within magmas effused to the surface (e.g., Hulme, 1973; Huppert and Sparks, 1985; Williams et al., 1998, 2000; Keszthelyi and Self, 1998; Sklar and Dietrich, 1998). The flow conditions and incision rates of Martian lavas with depths of up to 100 m have previously been investigated and suggest total mechanical and thermal incision rates of up to tens of meters per day for lavas flowing on nearly horizontal slopes underlain by bedrock (e.g., Jaeger et al., 2010; Hurwitz et al., 2010; Dundas and Keszthelyi, 2014; Hopper and Leverington, 2014; Cataldo et al., 2015; Baumgartner et al., 2017; Leverington, 2018, 2019a b; Dundas et al., 2019; Vetere et al., 2019; Gasparri et al., 2020).

On the basis of thermal considerations that involve maintenance of magma temperatures above those conducive to the incision of channels (Leverington, 2007, 2019a b; Cataldo et al., 2015), the minimum volume of lava required for formation of a Martian channel system should not be lower than ~8 times the channel volume. The total volume of material removed during formation of Ma'adim Vallis and its tributaries was ~14,000 km^3, and thus a minimum erupted lava volume of ~112,000 km^3 is implied for formation of this system. A larger erupted volume is expected for formation of Ma'adim Vallis, partly because lavas cannot all be expected to have been effused at sufficient volumes and rates to have efficiently incised highland terrain, and lower-volume eruptions have the potential to work against incision by constructively mantling channel systems.

Based on the results of Leverington (2018), generated to support investigation of Martian outflow system Kasei Valles, a discharge rate of ~4.2×10^6 m^3/s is estimated at Ma'adim Vallis for a flow depth of 20 m, a lava viscosity of 1 Pa s, a slope of 0.4°, and a 10 km channel width. Estimated incision rates for 20-m-deep flows on slopes of up to 1°, derived on the basis of the set of equations outlined by Hurwitz et al. (2010, 2012) and the parameters utilized by Leverington (2018, 2019 ab), are summarized in Fig. 10 for viscosities of 1–10,000 Pa s. For 20-m-deep lavas with viscosities as low as 1 Pa s and substrate slopes of up to 1°, mechanical incision rates in excess of 10 m/day are possible, as are thermal incision rates of almost 3 m/day. The incision rates of thermal and mechanical processes are presently calculated separately, but in nature these processes are likely to combine their effects in a synergistic manner. Regardless of the exact capacity for incision that combined thermal and mechanical processes might possess, net incision rates of several meters per day are reasonable and are sufficient for development of the largest Martian channels (e.g., Leverington, 2018, 2019a b), and smaller highland channel networks such as Ma'adim Vallis are similarly expected to be readily formed by voluminous effusions of low-viscosity lavas. Typical channel depths below adjacent highlands at Ma'adim Vallis range between ~700 m and 2300 m, and in a simplified scenario involving an average incision depth of 1500 m and a conservative net incision rate of 2 m/day, a total incision time of 750 days is estimated (involving an unknown number of events and an unknown total number of separate volcanic sources, and involving geological timescales likely dominated by periods of little to no local volcanic activity). With an assumed discharge rate of 4.2×10^6 m^3/s, a total erupted volume of 272,000 km^3 is estimated in this simplified scenario. This is approximately 2.5 times the minimum volume estimated above on the basis of simple thermal considerations, and is considered to be a more realistic estimate of the total volume of lava involved in the development of Ma'adim Vallis. Both volumes far exceed that of Gusev crater, confirming that most effused lavas interpreted to have been involved in channel incision would have necessarily been deposited in lowlands to the north of the system, requiring northward overflow of lavas and their local subsidence within Gusev crater; terrain located immediately north of Gusev crater suggests a complex history that partly involved later mantling by other volcanic flows and pyroclastic units (e.g., Scott and Tanaka, 1986; Kuzmin et al., 2000; Tanaka et al., 2014; Chuang et al., 2019), and lava subsidence within Gusev crater of ~300 m is suggested if modern topography in the area of the northwestern breach is simplistically assumed to approximate the topography that existed in the Late Noachian. Precise modeling of the manner in which Ma'adim Vallis might have been formed by lavas along its full length is hindered by the many unknowns involved, such as those related to the original character of regional topography in the Late Noachian, and those related to the number, location, and eruptive history of all relevant volcanic sources.

7. Discussion

For much of the past 40 years, it has been common practice to assume that most or all Martian channels were formed by aqueous flows, and that accumulations of geological materials at the mouths of these channels were likely deposited in ancient bodies of standing water. However, such assumptions are not warranted. Despite the existence of thousands of sites of aqueous alteration on Mars, the mineralogy of the planet's surface is remarkably pristine and overall has been little altered by water (e.g., Bibring et al., 2005, 2006; Hurowitz and McLennan, 2007; Christensen et al., 2008; Bibring and Langevin, 2008; Leverington, 2009, 2011, 2019a b; Ehlmann, 2014; Leone, 2014, 2018, 2020; Amador et al., 2018). Martian exposures of hydrated minerals are in many cases of limited extent and appear to be separated by vast tracts of little altered materials, and there is no special geographic correlation on Mars between hydrated minerals and channel systems of any kind (e.g., Bibring et al., 2006; Mangold et al., 2008; Carter et al., 2013; Wilson and Mustard, 2013; Ehlmann, 2014; Kaufman et al., 2019). There are no obvious near-shore or off-shore sedimentary deposits in the northern lowlands of Mars, nor are there expected levels of aqueous alteration or chemical sedimentation here (e.g., Ghatan and Zimbelman, 2006; Leverington, 2007, 2011, 2018,

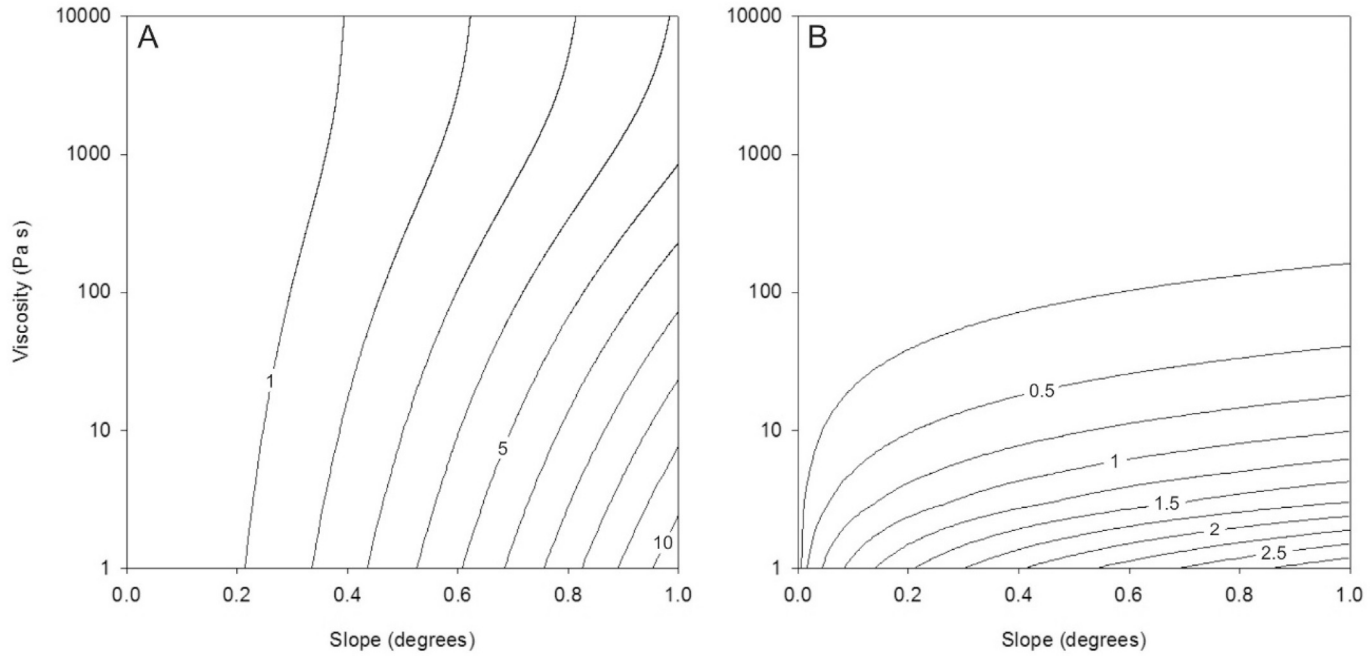

Fig. 10. Semi-log plots of estimated mechanical (A) and thermal (B) incision rates for Martian lava flows with depths of 20 m, based on the parameters and numerical model utilized in Leverington (2018, 2019 ab), using the equation set summarized by Hurwitz et al. (2010, 2012). Incision rates are given in meters per day for a lava temperature of 1350 °C and for a bedrock substrate. Contour increments are 1.0 m/day (*A*) and 0.25 m/day (*B*).

2019a b; Pretlow, 2013; Pan et al., 2017; Leone, 2014, 2018, 2020; Sholes et al., 2019). Proposed sites of ancient Martian lakes lack expected levels of aqueous alteration, lacustrine sedimentary deposits, and mantling by evaporites (e.g., Leverington and Maxwell, 2004; Leverington, 2005, 2006; Goudge et al., 2015; Gasparri et al., 2020). The many knickpoints, the common presence of hanging valleys, and the low basin concavities typical of Martian highland networks do not suggest channel development in association with prolonged erosion by aqueous surface runoff (Aharonson et al., 2002), and these attributes instead appear to be consistent with the dry origins independently suggested by the limited presence of local hydrous minerals. From a global perspective, the relatively pristine preservation of ancient olivine-rich materials on Mars (e.g., Hoefen et al., 2003; Rogers et al., 2005; Bibring et al., 2006; Koeppen and Hamilton, 2008; Ody et al., 2012b; Wilson and Mustard, 2013; Amador et al., 2018; Riu et al., 2019; Mandon et al., 2020) is arguably not consistent with the occurrence of younger periods of extensive wet conditions on this planet (e.g., Leverington, 2009, 2011, 2019a b; Leone, 2014, 2018, 2020).

Effusion of low-viscosity lavas on Mars can readily account for the existence and nature not only of the outflow channels (e.g., Leverington, 2004, 2007, 2009, 2011, 2014, 2018, 2019a b; Hopper and Leverington, 2014; Leone, 2014, 2017; Baumgartner et al., 2015, 2017), but also of the highland channel networks and associated topographic basins (e.g., Leverington and Maxwell, 2004; Leverington, 2005, 2006; Gasparri et al., 2020). Volcanic processes are especially attractive since they do not require unexpectedly large near-surface volatile reservoirs or high atmospheric pressures, and could operate under a wide variety of surface conditions including those of the present. In line with the above considerations, the existence and properties of Ma'adim Vallis can be most economically explained on the basis of the past operation of dry volcanic processes. Though there is no obvious evidence for the runoff and pooling of water at Ma'adim Vallis, there is abundant evidence for the past flow of low-viscosity lavas near the head of the system, along component channels, and at the system's mouth. Lavas with viscosities of ~1 Pa s have a clear capacity to incise large channel systems on Mars (e.g., Hopper and Leverington, 2014; Baumgartner et al., 2017; Leverington, 2018, 2019a b; Vetere et al., 2019; Gasparri et al., 2020), and such lavas are known to have accumulated near the mouth of Ma'adim Vallis (e.g., Gellert et al., 2004; Morris et al., 2004; Squyres et al., 2004; Greeley et al., 2005; Arvidson et al., 2006; Chevrel et al., 2014). Consistent with other channel systems in the region (e.g., Leverington and Maxwell, 2004), the character of Ma'adim Vallis is in line with dry development involving low-viscosity lavas that were erupted at numerous locales within surrounding uplands.

Is there any possibility that combined aqueous and volcanic development of Ma'adim Vallis occurred, with initial development of local channels by fluvial processes and later modification of these channels by volcanic resurfacing? Certainly, the volcanic modification of fluvial systems is possible in principle, and hybrid aqueous-volcanic mechanisms of channel development have previously been considered for large Martian systems such as Athabasca Valles and Kasei Valles (e.g., Jaeger et al., 2007, 2010; Dundas and Keszthelyi, 2014). If the duration of wet conditions in the Ma'adim Vallis region were orders of magnitude shorter than the millions of years previously hypothesized, and if involved waters were so pure as to not favor later deposition of evaporite minerals, this could correspondingly reduce the expected prominence of the mineralogical signatures of past aqueous environments. However, hydrous alteration of mafic and ultramafic lithologies can begin within only days of initial exposure to water (e.g., Baker et al., 2000), and, depending on the exact nature of local environmental conditions on Mars, alteration of mafic and ultramafic lithologies sufficient to show notable absorption features in reflectance spectra would likely require no more than years to millennia (e.g., Oze and Sharma, 2007; Hausrath et al., 2008). Consequently, even relatively short-lived lacustrine and fluvial conditions here should have produced more extensive swaths of hydrated materials than are evident. A hybrid aqueous-volcanic hypothesis for development of Ma'adim Vallis would therefore additionally seem to require the nearly complete erosion or mantling of expected hydrous materials in the region, in order to account for the relatively low level of alteration apparent at the surface today. Though parts of the Eridania basin region are relatively well exposed, some reaches of Ma'adim Vallis are indeed mantled today by anhydrous fines that obscure underlying materials (Figs. 4b and 5a). Uncertainties regarding the nature of buried geological units, and the continued support in the research community for aqueous

interpretations of the Ma'adim Vallis system, justify the future consideration of combined aqueous-volcanic origins for local channels. However, the fluvial, diluvial, and lacustrine processes previously hypothesized for development of this system, operating either alone or in concert with volcanic processes, arguably add considerable complexity without providing additional explanatory power. Volcanic accounts for the attributes of Ma'adim Vallis and the Eridania basin do not require postulation of the long-term persistence of regional or global aquifers, the voluminous pooling of water in large impact basins, the past occurrence of catastrophic aqueous floods, the past existence of high atmospheric pressures, and the erosion or mantling of all clear sedimentological and mineralogical evidence in support of the past operation of hypothesized fluvial and lacustrine processes.

The minimum lava volume estimated in this study to have been required for formation of Ma'adim Vallis is ~112,000 km^3, but a volume of several times this total is more likely to have been involved in system development. Though large in an absolute sense, such volumes are relatively small when compared to those believed to have been required for development of the most extensive Martian channel systems. For example, the outflow channels Kasei Valles and Ares Vallis are estimated to have required volcanic effusions of at least several million cubic kilometers for development of each system, or roughly the total original volume of some individual Large Igneous Provinces on Earth (Leverington, 2018, 2019b). Smaller Martian channel systems would have required correspondingly lower volumes of lava for development, with total volumes much closer to those estimated to have formed Ma'adim Vallis. For example, the Mangala Valles and Ravi Vallis outflow systems are estimated to have required minimum total erupted volumes of ~200,000 km^3 and 64,000 km^3, respectively (Leverington, 2007, 2019a), and the shallowly incised Athabasca Valles system is associated with an estimated lava volume of only ~7500 km^3 (Jaeger et al., 2010). For Martian channel systems of all sizes, reaches formed as a result of deep lava incision will very likely have required not only eruption of substantial volumes of lava, but also involvement of fluid viscosities of well under 100 Pa s (e.g., Leverington, 2019b).

Recognition of a volcanic origin for Ma'adim Vallis resolves past incompatibilities between aqueous interpretations of this system and the findings of the Spirit mission (Leverington, 2011), which revealed that deposits accumulated near the mouth of the system are mainly volcanic in character and lack obvious evidence for deposition in past lacustrine environments (e.g., Squyres et al., 2004). In a similar manner, the otherwise perplexing properties of the Viking 1 and Pathfinder landing sites are resolved through recognition of the volcanic origins for channels that terminate near these sites, including the Kasei Valles, Maja Valles, and Ares Vallis systems (e.g., Leverington, 2011, 2018, 2019b). The style of dry channel development at Ma'adim Vallis, involving effusion of low-viscosity lavas from multiple highland sources not necessarily marked by large areas of disturbed terrain, is only different from that involved in formation of outflow systems with regard to the generally less pronounced surface expression of involved volcanic plumbing systems. The style of volcanism involved in the formation of Ma'adim Vallis is expected to have been comparable to that which drove development of nearby systems such as Al-Qahira Vallis and Durius Valles, as well as many other highland channel networks on Mars (e.g., Leverington and Maxwell, 2004; Leverington, 2005, 2006, 2011; Leone, 2014, 2020; Gasparri et al., 2020).

Dry origins for Martian highland channel networks are arguably further supported by recent difficulties in determining realistic driving mechanisms for the warming events and high atmospheric pressures required for aqueous development of channels by precipitation (Wordsworth, 2016). Such dry origins may also be congruous with the basic nature of features previously considered to be good evidence for otherwise unexpectedly large volumes of near-surface volatiles on Mars, such as some impact features. Fluidized ejecta blankets with distinct lobate margins have previously been interpreted as possible products of water-rich slurries produced by the heating of ice-rich materials during impacts (e.g., Mouginis-Mark, 1981; Lucchitta, 1985; Costard, 1989), but the absence of hydrated minerals at well-exposed examples of these ejecta blankets such as those within the Nili Patera caldera floor has instead suggested their emplacement as dry lavas (Bibring and Langevin, 2008); similar fluidized ejecta deposits are known for impact craters on Venus (e.g., Phillips et al., 1991; You et al., 1995), independently suggesting that formation of Martian fluidized ejecta blankets need not have involved the melting of ground ice.

Overall, volcanic development of highland channel networks such as Ma'adim Vallis is consistent with a wide range of geomorphological and mineralogical attributes of the Martian surface, some of which are entirely independent of the channels themselves. If valid, a volcanic origin for highland channel networks further diminishes the role of flowing water in the past development of Martian landscapes. Dry origins for both the Martian outflow channels and highland networks would bring estimates of surface and near-surface water contents back in line with geochemical expectations and direct observations, and reduce or eliminate the need to hypothesize past periods characterized by unexpectedly thick atmospheres and wet surface conditions (e.g., Leverington, 2009, 2011, 2019a b; Leone, 2014, 2018, 2020).

8. Conclusions

Ma'adim Vallis has previously been interpreted as a product of aqueous incision by long-term surface runoff, sapping, and/or catastrophic overflows from lakes. Aqueous interpretations of this channel system have led to past hypotheses that water was once ponded within Gusev crater, within topographic basins located along the main channel of the system, and within adjacent basins of the northern lowlands and southern highlands. A widely held interpretation of Ma'adim Vallis involves channel development near the end of the Noachian as a result of catastrophic drainage of a large and long-lived lake in the Eridania basin. Problematically, obvious examples of fluvial or lacustrine sedimentary deposits have proven difficult to identify at Ma'adim Vallis and associated basins. Instead, many features related to this channel system have appearances and properties aligned with volcanic origins. Most notably, basins and channels are widely mantled in the Ma'adim Vallis region by ridged plains that have basic characteristics similar to those of lunar flood lavas.

Much of Ma'adim Vallis is blanketed by fines that partly obscure the mineralogy of underlying materials, but the mouth region of the system at Gusev crater is known from *in situ* exploration conducted by the Spirit rover to be substantially mantled by mineralogically pristine volcanic flows of Hesperian age. The nature of aqueous alteration of Noachian-aged materials in the Columbia Hills confirms the past action of local hydrothermal processes but is not suggestive of past lacustrine conditions here, and the mineralogical properties of the Eridania basin contradict the hypothesized long-term existence of an enormous and long-lived lake that suddenly released a proportion of its volume in northbound floods and lost its remaining waters through evaporation or sublimation in closed basins. Instead, the most economical interpretation of landforms and surface materials associated with the Ma'adim Vallis system is that hypothesized lacustrine environments have never existed at Gusev crater or inside the Eridania basin.

The properties of Ma'adim Vallis are most consistent with dry volcanic origins involving effusions of low-viscosity flood lavas from multiple highland sources primarily during the Noachian and Hesperian. Though most of the volcanic sources involved in eruption of these lavas are expected to be buried, candidate examples of exposed volcanic sources include the graben-like structures of Sirenum Fossae and other Tharsis-radial structural features in the region. Parts of the Intermediate basin of Ma'adim Vallis are characterized by the presence of ridged plains of a character similar to that of the plains at Gusev crater and within the Eridania basin, suggesting emplacement here of analogous low-viscosity lava flows from sources located both inside and outside of local impact craters. The channels that extend from some of these craters suggest

incision by associated lavas during periods of overflow, which must necessarily have been followed by decreases in lava levels, presumably as a result of processes such as lava drainback into igneous intrusions.

A discharge rate of ~4.2 × 10^6 m^3/s is estimated at Ma'adim Vallis for flow depths of 20 m, lava viscosities of 1 Pa s, slopes of 0.4°, and 10 km channel widths. For 20-m-deep lavas with viscosities as low as 1 Pa s and substrate slopes of up to 1°, mechanical incision rates in excess of 10 m/day and thermal incision rates of almost 3 m/day are possible. Total incision rates of several meters per day are in line with past incision estimates made for other volcanic channels of the inner solar system, and could realistically have led to development of Ma'adim Vallis and other highland channel networks on Mars. A minimum total erupted lava volume of ~112,000 km^3 is estimated for formation of Ma'adim Vallis, but a larger total volume is likely since not all lavas can be assumed to have been erupted under conditions promoting efficient channel incision. Dry volcanic development of Ma'adim Vallis resolves the otherwise perplexing character of Gusev crater materials, bringing the findings of the Spirit mission into accord with channel origins.

CRediT authorship contribution statement

David W. Leverington: Conceptualization, Formal analysis, Investigation, Methodology, Software, Validation, Visualization, Writing - original draft, Writing - review & editing.

Declaration of competing interest

The authors declare that they have no known competing financial interests or personal relationships that could have appeared to influence the work reported in this paper.

Acknowledgements

The helpful comments of two anonymous reviewers are appreciated.

Appendix A. Supplementary data

Supplementary data to this article can be found online at https://doi.org/10.1016/j.pss.2020.105021.

References

Adeli, S., Hauber, E., Le Deit, L., Jaumann, R., 2015. Geologic evolution of the eastern Eridania basin: implications for aqueous processes in the southern highlands of Mars. J. Geophys. Res. 120, 1774–1799.

Aharonson, O., Zuber, M.T., Rothman, D.H., Schorghofer, N., Whipple, K.X., 2002. Drainage basins and channel incision on Mars. Proc. Natl. Acad. Sci. U.S.A. 99, 1780–1783.

Amador, E.S., Bandfield, J.L., Thomas, N.H., 2018. A search for minerals associated with serpentinization across Mars using CRISM spectral data. Icarus 311, 113–134.

Anderson, R.C., Dohm, J.M., Williams, J.P., Robbins, S.J., Siwabessy, A., Golombek, M.P., Schroeder, J.F., 2019. Unraveling the geologic and tectonic history of the Memnonia-Sirenum region of Mars: implications on the early formation of the Tharsis rise. Icarus 332, 132–150.

Andrews-Hanna, J.C., Phillips, R.J., Zuber, M.T., 2007. Meridiani planum and the global hydrology of mars. Nature 446, 163–166. https://doi.org/10.1038/nature005594.

Arvidson, R.E., et al., 2006. Overview of the Spirit mars exploration rover mission to Gusev crater: landing site to backstay rock in the Columbia Hills. J. Geophys. Res. 111, E02S01. https://doi.org/10.1029/2005JE002499.

Baker, D.M., Head, J.W., 2009. The origin of Eridania Lake and Ma'adim Vallis: an investigation of closed chaos basins, Hesperian ridged plains, and tectonic constructs on the floor of a large hypothesized paleolake on Mars. In: Proc. Lunar Planet. Sci. Conf. 40th. Houston, TX, Abstract 1835.

Baker, D.M.H., Head, J.W., 2012. Geology and chronology of the Ma'adim Vallis – Eridania basin region, mars: implications for the noachian – hesperian hydrological cycle. In: Proc. Lunar Planet. Sci. Conf. 43rd. Houston, TX, Abstract 1252.

Baker, L.L., Agenbroad, D.J., Wood, S.A., 2000. Experimental hydrothermal alteration of a martian analog basalt: implications for martian meteorites. Meteoritics Planet Sci. 35, 31–38.

Baker, V.R., 1982. The Channels of Mars. University of Texas Press, Austin TX.

Baker, V.R., Milton, D.J., 1974. Erosion by catastrophic floods on mars and Earth. Icarus 23, 27–41.

Baker, V.R., Kochel, R.C., 1978a. Morphological mapping of martian outflow channels. Proc. Lunar Planet Sci. Conf. 9th, 3181–3192.

Baker, V.R., Kochel, R.C., 1978b. Morphometry of streamlined forms in terrestrial and martian channels. Proc. Lunar Planet Sci. Conf. 9th, 3193–3203.

Baker, V.R., et al., 1991. Ancient oceans, ice sheets, and the hydrological cycle on Mars. Nature 352, 589–594.

Baker, V.R., Komatsu, G., Parker, T.J., Gulick, V.C., Kargel, J.S., Lewis, J.S., 1992. Channels and valleys on Venus: preliminary analysis of Magellan data. J. Geophys. Res. 97 (13), 421-13,444.

Baker, V.R., Komatsu, G., Gulick, V.C., Parker, T.J., 1997. Channels and valleys. In: Bougher, S.W., Hunten, D.M., Phillips, R.J. (Eds.), Venus II. Univ. of Ariz. Press, Tucson, AZ, pp. 757–793.

Barnes, S.J., 2006. Komatiite-hosted Nickel Sulfide Deposits: Geology, Geochemistry, and Genesis, vol. 13. Society of Economic Geologists, Special Publication, pp. 51–97.

Baumgartner, R.J., Fiorentini, M.L., Baratoux, D., Micklethwaite, S., Sener, A.K., Lorand, J.P., McCuaig, T.C., 2015. Magmatic controls on the genesis of Ni-Cu-(PGE) sulphide mineralisation on Mars. Ore Geol. Rev. 65, 400–412.

Baumgartner, R.J., Baratoux, D., Gaillard, F., Fiorentini, M.L., 2017. Numerical modeling of erosion and assimilation of sulfur-rich substrate by martian lava flows: implications for the genesis of massive sulfide mineralization on Mars. Icarus 296, 257–274.

Bibring, J.-P., Langevin, Y., Gendrin, A., Gondet, B., Poulet, F., Berthé, M., Soufflot, A., Arvidson, R., Mangold, N., Mustard, J., Drossart, P., Omega Team, 2005. Mars surface diversity as revealed by the OMEGA/Mars Express Observations. Science 307, 1576–1581.

Bibring, J.-P., Langevin, Y., Mustard, J.F., Poulet, F., Arvidson, R., Gendrin, A., Gondet, B., Mangold, N., Pinet, P., Forget, F., Omega Team, 2006. Global mineralogical and aqueous mars history derived from OMEGA/Mars Express data. Science 312, 400–404.

Bibring, J.-P., Langevin, Y., 2008. Mineralogy of the martian surface from mars express OMEGA observations. Chapter 7 in "the martian surface – composition, mineralogy, and physical properties". In: Bell, J. (Ed.), Cambridge Planetary Science. Cambridge University Press, New York, pp. 153–168.

Brakenridge, G.R., 1990. The origin of fluvial valleys and early geologic history, Aeolis Quadrangle, Mars. J. Geophys. Res. 95 (17), 289-17,308.

Brož, P., Hauber, E., Platz, T., Balme, M., 2015. Evidence for Amazonian highly viscous lavas in the southern highlands on Mars. Earth Planet Sci. Lett. 415, 200–212.

Byrne, P.K., Klimczak, C., Williams, D.A., Hurwitz, D.M., Solomon, S.C., Head, J.W., Preusker, F., Oberst, J., 2013. An assemblage of lava flow features on Mercury. J. Geophys. Res. 118, 1303–1322. https://doi.org/10.1002/jgre.20052.

Cabrol, N.A., Grin, E.A., 2001. The evolution of lacustrine environments on Mars: is Mars only hydrologically dormant? Icarus 149, 291–328.

Cabrol, N.A., Landheim, R., Greeley, R., Farmer, J., 1994. Fluvial processes in Ma'adim Vallis and the potential of Gusev crater as a high priority site. In: Proc. Lunar Planet. Sci. Conf. 25th, pp. 213–214. Houston, TX.

Cabrol, N.A., Grin, E.A., Dawidowicz, G., 1996. Ma'adim Vallis revisited through new topographic data: evidence for an ancient intravalley lake. Icarus 123, 269–283.

Cabrol, N.A., Landheim, R., Grin, E.A., 1997. Ma'adim Vallis paleocourses. In: Proc. Lunar Planet. Sci. Conf. 28th. Houston, TX, Abstract 1026.

Cabrol, N.A., Grin, E.A., Landheim, R., 1998a. Ma'adim Vallis evolution: geometry and models of discharge rate. Icarus 132, 362–377.

Cabrol, N.A., Grin, E.A., Landheim, R., Kuzmin, R.O., Greeeley, R., 1998b. Duration of the Ma'adim Vallis/Gusev crater hydrogeologic system, mars. Icarus 133, 98–108.

Cabrol, N.A., Grin, E.A., Landheim, R., Greeley, R., Kuzmin, R.O., 1999. About the 'non-evidence' of a paleolake in Gusev crater, Mars. In: Proc. Lunar Planet. Sci. Conf. 30th. Houston, TX, Abstract 1030.

Campbell, B.A., Clark, D.A., 2006. Geologic map of the mead quadrangle (V-21), Venus. Atlas of Venus: mead quadrangle. U.S. Geol. Surv. Sci. Invest. Map 2897.

Capitan, R.D., Van De Wiel, M., 2011. Landform hierarchy and evolution in Gorgonum and Atlantis basins, mars. Icarus 211, 366–388.

Carr, M.H., 1979. Formation of Martian flood features by release of water from confined aquifers. J. Geophys. Res. 84, 2995–3007.

Carr, M.H., 1996. Water on Mars. Oxford University Press, New York, p. 229.

Carr, M.H., 2012. The fluvial history of Mars. Philos. Trans. R. Soc. London, Ser. A 370, 2193–2215.

Carr, M.H., Head, J.W., 2015. Martian surface/near-surface water inventory: sources, sinks, and changes with time. Geophys. Res. Lett. https://doi.org/10.1002/2014GL062464.

Carter, B.L., Frey, H., Sakimoto, S.E.H., Roark, J., 2001. Constraints on Gusev basin infill from the mars orbiter laser altimeter (MOLA) topography. In: Proc. Lunar Planet. Sci. Conf. 32nd. Houston, TX, Abstract 2042.

Carter, J., Poulet, F., 2012. Orbital identification of clays and carbonates in Gusev crater. Icarus 219, 250–253.

Carter, J., Poulet, F., Bibring, J.-P., Mangold, N., Murchie, S., 2013. Hydrous minerals on Mars as seen by CRISM and OMEGA imaging spectrometers: updated global view. J. Geophys. Res. 118, 831–858.

Cataldo, V., Williams, D.A., Dundas, C.M., Keszthelyi, L.P., 2015. Limited role for thermal erosion by turbulent lava in proximal Athabasca Valles, Mars. J. Geophys. Res. 120, 1800–1819.

Chapman, M.G., Neukum, G., Dumke, A., Michael, G., van Gasselt, S., Kneissl, T., Zuschneid, W., Hauber, E., Ansan, V., Mangold, N., Masson, P., 2010a. Noachian-hesperian geologic history of the echus chasma and Kasei Valles system on mars: new data and interpretations. Earth Planet Sci. Lett. 294, 256–271.

Chapman, M.G., Neukum, G., Dumke, A., Michael, G., van Gasselt, S., Kneissl, T., Zuschneid, W., Hauber, E., Mangold, N., 2010b. Amazonian geologic history of the

echus chasma and Kasei Valles system on mars: new data and interpretations. Earth Planet Sci. Lett. 294, 238–255.
Chevrel, M.O., Baratoux, D., Hess, K.-U., Dingwell, D.B., 2014. Viscous flow behavior of tholeiitic and alkaline Fe-rich martian basalts. Geochem. Cosmochim. Acta 124, 348–365.
Christensen, P.R., Bandfield, J.L., Hamilton, V.E., Ruff, S.W., Kieffer, H.H., Titus, T.N., Malin, M.C., Morris, R.V., Lane, M.D., Clark, R.L., Jakosky, B.M., Mellon, M.T., Pearl, J.C., Conrath, B.J., Smith, M.D., Clancy, R.T., Kuzmin, R.O., Roush, T., Mehall, G.L., Gorelick, N., Bender, K., Murray, K., Dason, S., Greene, E., Silverman, S., Greenfield, M, 2001. Mars Global Surveyor Thermal Emission Spectrometer experiment: investigation description and surface science results. J. Geophys. Res. 106. E10, 23,823-23,871.
Christensen, P.R., Bandfield, J.L., Rogers, A.D., Glotch, T.D., Hamilton, V.E., Ruff, S.W., Wyatt, M.B., 2008. Global mineralogy mapped from the mars global surveyor thermal emission spectrometer. Chapter 9 in "the martian surface – composition, mineralogy, and physical properties". In: Bell, J. (Ed.), Cambridge Planetary Science. Cambridge University Press, New York, pp. 195–220.
Christensen, P.R., Fergason, R.L., 2013. THEMIS-derived thermal inertia mosaic of Mars: product description and science results. In: Proc. Lunar Planet. Sci. Conf. 44th. Houston, TX, Abstract 2822.
Chuang, F.C., Crown, D.A., Berman, D.C., 2019. Geology of the northeastern flank of Apollinaris Mons, Mars: constraints on the erosional history from morphology, topography, and crater populations. Icarus 333, 385–403.
Costard, F.M., 1989. The spatial distribution of volatiles in the Martian hydrolithosphere. Earth, Moon, and Planets 45, 265–290.
Davila, A.F., Gross, C., Marzo, G.A., Fairén, A.G., Kneissl, T., McKay, C.P., Dohm, J.M., 2011. A large sedimentary basin in the Terra Sirenum region of the southern highlands of Mars. Icarus 212, 579–589.
de Pablo, M.A., Fairén, A.G., 2004. Atlantis basin, Sirenum Terrae, Mars: geological setting and astrobiological implications. Int. J. Astrobiol. 3, 257–263.
Dundas, C.M., Keszthelyi, L.P., 2014. Emplacement and erosive effects of lava in south Kasei Valles, Mars. J. Volcanol. Geoth. Res. 282, 92–102.
Dundas, C.M., Cushing, G.E., Keszthelyi, L.P., 2019. The flood lavas of Kasei Valles, mars. Icarus 321, 346–357.
Edwards, C.S., Bandfield, J.L., Christensen, P.R., Fergason, R.L., 2009. Global distribution of bedrock exposures on Mars using THEMIS high-resolution thermal inertia. J. Geophys. Res. 114, E11001. https://doi.org/10.1029/2009JE003363.
Edwards, C.S., Bandfield, J.L., Christensen, P.R., Rogers, A.D., 2014. The formation of infilled craters on Mars: evidence for widespread impact induced decompression of the early martian mantle? Icarus 228, 149–166.
Ehlmann, B.L., 2014. The first billion years – warm and wet vs. cold and ice? Eighth Int. Conf. on Mars. Pasadena, CA, Abstract 1245.
Fairén, A.G., Davila, A.F., Gago-Duport, L., Haqq-Misra, J.D., Gil, C., McKay, C.P., Kasting, J.F., 2011. Cold glacial oceans would have inhibited phyllosilicate sedimentation on early Mars. Nat. Geosci. 4, 667–670.
Fassett, C.I., Head III, J.W., 2008. Valley network-fed, open-basin lakes on Mars: distribution and implications for Noachian surface and subsurface hydrology. Icarus 198, 37–56.
Gasparri, D., Leone, G., Cataldo, V., Punjabi, V., Nandakumar, S., 2020. Lava filling of gale crater from tyrrhenus Mons on mars. J. Volcanol. Geoth. Res. 389, 106743.
Gellert, R., et al., 2004. Chemistry of rocks and soils in Gusev crater from the alpha particle X-ray spectrometer. Science 305, 829–832.
Ghatan, G.J., Zimbelman, J.R., 2006. Paucity of candidate coastal constructional landforms along proposed shorelines on Mars: implications for a northern lowlands-filling ocean. Icarus 185, 171–196.
Gillis-Davis, J.J., Blewett, D.T., Gaskell, R.W., Denevi, B.W., Robinson, M.S., Strom, R.G., Solomon, S.C., Sprague, A.L., 2009. Pit-floor craters on Mercury: evidence of near-surface igneous activity. Earth Planet Sci. Lett. 285, 243–250.
Glotch, T.D., Bandfield, J.L., Tornabene, L.L., Jensen, H.B., Seelos, F.P., 2010. Distribution and formation of chlorides and phyllosilicates in Terra Sirenum, mars. Geophys. Res. Lett. 37, L16202. https://doi.org/10.1029/2010GL044557.
Goldspiel, J.M., Squyres, S.W., 1991. Ancient aqueous sedimentation on Mars. Icarus 89, 392–410.
Gole, M.J., Robertson, J., Barnes, S.J., 2013. Extrusive origin and structural modification of the komatiitic Mount Keith ultramafic unit. Econ. Geol. 108, 1731–1752.
Golombek, M.P., et al., 2005. Assessments of mars exploration rover landing site predictions. Nature 436, 44–48.
Gornitz, V., 1973. The origin of sinuous rilles. Moon 6, 337–356.
Goudge, T.A., Mustard, J.F., Head, J.W., Fassett, C.I., 2012. Constraints on the history of open-basin lakes on Mars from the composition and timing of volcanic resurfacing. J. Geophys. Res. 117, E00J21. https://doi.org/10.1029/2012JE004115.
Goudge, T.A., Aureli, K.L., Head, J.W., Fassett, C.I., Mustard, J.F., 2015. Classification and analysis of candidate impact crater-hosted closed-basin lakes on Mars. Icarus 260, 346–367.
Goudge, T.A., Fassett, C.I., Mohrig, D., 2018. Incision of paleolake outlet canyons on Mars from overflow flooding. Geology 47, 7–10.
Grant, J.A., Schultz, P.H., 1990. Gradational epochs on mars: evidence from west-northwest of Isidis basin and Electris. Icarus 84, 166–195.
Grant, J.A., et al., 2004. Surficial deposits at Gusev crater along Spirit rover traverses. Science 305, 807–810.
Grant, J.A., Wilson, S.A., Noe Dobrea, E., Fergason, R.L., Griffes, J.L., Moore, J.M., Howard, A.D., 2010. HiRISE views enigmatic deposits in the Sirenum Fossae region of Mars. Icarus 205, 53–63.
Greeley, R., 1971. Lunar hadley rille: considerations of its origin. Science 172, 722–725.
Greeley, R., Fagents, S.A., Harris, R.S., Kadel, S.D., Williams, D.A., 1998. Erosion by flowing lava: field evidence. J. Geophys. Res. 103 (27), 325-327,345.
Greeley, R., Foing, B.H., McSween Jr., H.Y., Neukum, G., Pinet, P., van Kan, M., Werner, S.C., Williams, D.A., Zegers, T.E., 2005. Fluid lava flows in Gusev crater, Mars. J. Geophys. Res. 110, E05008. https://doi.org/10.1029/20005JE002401.
Greeley, R., Guest, J.E., 1987. Geologic map of the eastern equatorial region of mars. IMAP 1. https://doi.org/10.3133/i1802B, 5 000 000.
Grin, E.A., Cabrol, N.A., 1997. Limnologic analysis of Gusev crater paleolake, Mars. Icarus 130, 461–474.
Gulick, V.C., 2001. Origin of the valley networks on Mars: a hydrological perspective. Geomorphology 37, 241–268.
Hamilton, C.W., Mouginis-Mark, P.J., Sori, M.M., Scheidt, S.P., Bramson, A.M., 2018. Episodes of aqueous flooding and effusive volcanism associated with Hrad Vallis, Mars. J. Geophys. Res. 123, 1484–1510.
Hartmann, W.K., 2005. Martian cratering 8: isochron refinement and the chronology of Mars. Icarus 174, 294–320.
Hartmann, W.K., Anguita, J., de la Casa, M.A., Berman, D.C., Ryan, E.V., 2001. Martian cratering 7: the role of impact gardening. Icarus 149, 37–53.
Haskin, L.A., Wang, A., Jolliff, B.L., McSween, H.Y., Clark, B.C., Des Marais, D.J., McLennan, S.M., Tosca, N.J., Hurowitz, J.A., Farmer, J.D., Yen, A., Squyres, S.W., Arvidson, R.E., Klingelhofer, G., Schroder, C., de Souza, P.A., Ming, D.W., Gellert, R., Zipfel, J., Bruckner, J., Bell, J.F., Herkenhoff, K., Christensen, P.R., Ruff, S., Blaney, D., Gorevan, S., Cabrol, N.A., Crumpler, L., Grant, J., Soderblom, L., 2005. Water alteration of rocks and soils on Mars at the Spirit rover site in Gusev crater. Nature 436, 66–69.
Hausrath, E.M., Navarre-Sitchler, A.K., Sak, P.B., Steefel, C.I., Brantley, S.L., 2008. Basalt weathering rates on Earth and the duration of liquid water on the plains of Gusev Crater, Mars. Geology 36, 67–70.
Head III, J.W., Crumpler, L.S., Aubele, J.C., Guest, J.E., Saunders, R.S., 1992. Venus volcanism: classification of volcanic features and structures, associations, and global distribution from Magellan data. J. Geophys. Res. 97 (13), 153-13,197.
Head, J.W., Chapman, C.R., Strom, R.G., Fassett, C.I., Denevi, B.W., Blewett, D.T., Ernst, C.M., Watters, T.R., Solomon, S.C., Murchie, S.L., Prockter, L.M., Chabot, N.L., Gillis-Davis, J.J., Whitten, J.L., Goudge, T.A., Baker, D.M.H., Hurwitz, D.M., Ostrach, L.R., Xiao, Z., Merline, W.J., Kerber, L., Dickson, J.L., Oberst, J., Byrne, P.K., Klimczak, C., Nittler, L.R., 2011. Flood volcanism in the northern high latitudes of Mercury revealed by MESSENGER. Science 333, 1853–1856.
Head, J., Forget, F., Wordsworth, R., Turbet, M., Cassanelli, J., Palumbo, A., 2018. Two oceans on Mars?: history, problems, and prospects. In: Proc. Lunar Planet. Sci. Conf. 49th. Houston, TX, Abstract 2194.
Hills, J.M., 1984. Sedimentation, tectonism, and hydrocarbon generation in the Delaware basin, west Texas and southeastern New Mexico. American Association of Petroleum Geology Bulletin 68, 250–267.
Hoefen, T.M., Clark, R.N., Bandfield, J.L., Smith, M.D., Pearl, J.C., Christensen, P.R., 2003. Discovery of olivine in the Nili Fossae region of mars. Science 302, 627–630.
Hopper, J.P., Leverington, D.W., 2014. Formation of Hrad Vallis (Mars) by low viscosity lava flows. Geomorphology 207, 96–113.
Houlé, M.G., Gibson, H.L., Lesher, C.M., Davis, P.C., Cas, R.A.F., Beresford, S.W., Arndt, N.T., 2008. Komatiitic sills and multigenerational peperite at dundonald beach, abitibi greenstone belt, ontario: volcanic architecture and nickel sulfide distribution. Econ. Geol. 103, 1269–1284.
Houlé, M.G., Lesher, M., Davis, P.C., 2012. Thermomechanical erosion at the Alexo Mine, Abitibi greenstone belt, Ontario: implications for the genesis of komatiite-associated Ni-Cu-(PGE) mineralization. Miner. Deposita 47, 105–128.
Howard, A.D., Moore, J.M., 2004. Scarp-bounded benches in Gorgonum chaos, mars: formed beneath an ice-covered lake? Geophys. Res. Lett. 31, L01702. https://doi.org/10.1029/2003GL018925.
Howard, A.D., Moore, J.M., 2011. Late hesperian to early amazonian midlatitude martian valleys: evidence from Newton and Gorgonum basins. J. Geophys. Res. 116, E05003. https://doi.org/10.1029/2010JE003782.
Hulme, G., 1973. Turbulent lava flow and the formation of lunar sinuous rilles. Mod. Geol. 4, 107–117.
Hulme, G., 1982. A review of lava flow processes related to the formation of lunar sinuous rilles. Geophys. Surv. 5, 245–279.
Hulme, G., Fielder, G., 1977. Effusion rates and rheology of lunar lavas. Philos. Trans. R. Soc. London, Ser. A 285, 227–234.
Huppert, H.E., Sparks, R.S.J., Turner, J.S., Arndt, N.T., 1984. Emplacement and cooling of komatiite lavas. Nature 309, 19–22.
Huppert, H.E., Sparks, R.S.J., 1985. Cooling and contamination of mafic and ultramafic magmas during ascent through continental crust. Earth Planet Sci. Lett. 74, 371–386.
Hurowitz, J.A., McLennan, S.M., 2007. A ~3.5 Ga record of water-limited, acidic weathering conditions on Mars. Earth Planet Sci. Lett. 260, 432–443.
Hurwitz, D.M., Fassett, C.I., Head, J.W., Wilson, L., 2010. Formation of an eroded lava channel within an Elysium Planitia impact crater: distinguishing between a mechanical and thermal origin. Icarus 210, 626–634.
Hurwitz, D.M., Head, J.W., Wilson, L., Hiesinger, H., 2012. Origin of lunar sinuous rilles: modeling effects of gravity, surface slope, and lava composition on erosion rates during the formation of Rima Prinz. J. Geophys. Res. 117, E00H14. https://doi.org/10.1029/2011JE004000.
Hurwitz, D.M., Head, J.W., Hiesinger, H., 2013a. Lunar sinuous rilles: distribution, characteristics, and implications for their origin. Planet. Space Sci. 79–80, 1–38.
Hurwitz, D.M., Head, J.W., Byrne, P.K., Xiao, Z., Solomon, S.C., Zuber, M.T., Smith, D.E., Neumann, G.A., 2013b. Investigating the origin of candidate lava channels on Mercury with MESSENGER data: theory and observations. J. Geophys. Res. 118, 471–486.
Irwin, R.P., Maxwell, T.A., Howard, A.D., Craddock, R.A., Leverington, D.W., 2002. A large paleolake basin at the head of Ma'adim Vallis, Mars. Science 296, 2209–2212.

Irwin, R.P., Howard, A.D., Maxwell, T.A., 2004. Geomorphology of Ma'adim Vallis, Mars, and associated paleolake basins. J. Geophys. Res. 109, E12009. https://doi.org/10.1029/2004JE002287.
Irwin, R.P., Tanaka, K.L., Robbins, S.J., 2013. Distribution of early, middle, and late Noachian cratered surfaces in the Martian highlands: implications for resurfacing events and processes. J. Geophys. Res. 118, 278–291.
Ivanov, M.A., Head, J.W., 2013. The history of volcanism on Venus. Planet. Space Sci. 84, 66–92.
Ivanov, M.A., Hiesinger, H., Erkeling, G., Hielscher, F.J., Reiss, D., 2012. Major episodes of geologic history of Isidis planitia on mars. Icarus 218, 24–46.
Jaeger, W.L., Keszthelyi, L.P., McEwen, A.S., Dundas, C.M., Russell, P.S., 2007. Athabasca Valles: a lava-draped channel system. Science 317, 1709–1711.
Jaeger, W.L., Keszthelyi, L.P., Skinner Jr., J.A., Milazzo, M.P., McEwen, A.S., Titus, T.N., Rosiek, M.R., Galuszka, D.M., Howington-Kraus, E., Kirk, R.L., HiRISE Team, 2010. Emplacement of the youngest flood lava on Mars: a short, turbulent story. Icarus 205, 230–243.
Kargel, J.S., Komatsu, G., Baker, V.R., Strom, R.G., 1993. The volcanology of Venera and VEGA landing sites and the geochemistry of Venus. Icarus 103, 253–275.
Kaufman, S.V., Mustard, J.F., Head, J.W., 2019. Valley networks and hydrous mineralogy: quantifying the inverse spatial correlation between features formed by liquid water. In: Proc. Lunar Planet. Sci. Conf. 50th. Houston, TX, Abstract 2207.
Kaula, W.M., Schubert, G., Lingenfelter, R.E., Sjogren, W.L., Wollenhaupt, W.R., 1973. Lunar topography from Apollo 15 and 16 laser altimetry. In: Proceedings of the Fourth Lunar Science Conference, Supplement 4: Geochim. Cosmochim. Acta, vol. 3, pp. 2811–2819.
Keszthelyi, L., Self, S., 1998. Some physical requirements for the emplacement of long basaltic lava flows. J. Geophys. Res. 103 (27), 447-27,464.
Keszthelyi, L., McEwan, A.S., Thordarson, T., 2000. Terrestrial analogs and thermal models for Martian flood lavas. J. Geophys. Res. 105 (15), 027-15,049.
Keszthelyi, L., Thordarson, T., McEwen, A., Haack, H., Guilbaud, M.-N., Self, S., Rossi, M.J., 2004. Icelandic analogs to Martian flood lavas. Geochem. Geophys. Geosyst. 5 https://doi.org/10.1029/2004GC0000758.
Kleinhans, M.G., 2005. Flow discharge and sediment transport models for estimating a minimum timescale of hydrological activity and channel and delta formation on Mars. J. Geophys. Res. 110, E12003. https://doi.org/10.1029/2005JE002521.
Koeppen, W.C., Hamilton, V.E., 2008. Global distribution, composition, and abundance of olivine on the surface of Mars from thermal infrared data. J. Geophys. Res. 113, E05001. https://doi.org/10.1029/2007JE002984.
Komatsu, G., 2007. Rivers in the Solar System: water is not the only fluid flow on planetary bodies. Geography Compass 1, 480–502.
Komatsu, G., Baker, V.R., Gulick, V.C., Parker, T.J., 1993. Venusian channels and valleys distribution and volcanological implications. Icarus 102, 1–25.
Krijgsman, W., Hilgen, F.J., Raffi, I., Sierro, F.J., Wilson, D.S., 1999. Chronology, causes and progression of the Messinian salinity crisis. Nature 400, 652–655.
Kuzmin, R.O., Greeley, R., Landheim, R., Cabrol, N.A., Farmer, J.D., 2000. Geologic map of the MTM-15182 and MTM-15187 quadrangles, Gusev crater – Ma'adim Vallis region, Mars. U.S. Geol. Surv., Geol. Invest. Ser. Map I-2666.
Landheim, R., 1995. Exobiology Sites for Mars Exploration and Geologic Mapping of Gusev Crater – Ma'adim Vallis. Arizona State University, Tempe, p. 167.
Landheim, R., Cabrol, N.A., Farmer, J.D., 1994. Stratigraphic assessment of Gusev crater as an exobiology landing site. In: Proc. Lunar Planet. Sci. Conf. 25th, pp. 769–770. Houston, TX.
Larsen, I.J., Lamb, M.P., 2016. Progressive incision of the Channeled Scablands by outburst floods. Nature 538, 229–232.
Leask, E.K., Ehlmann, B.L., Anderson, R., Wray, J.J., 2017. Martian lake plumbing: mineralogy, morphology, and geologic context of hydrated minerals in Terra Sirenum. In: Proc. Lunar Planet. Sci. Conf. 48th. Houston, TX, Abstract 2609.
Leone, G., 2014. A network of lava tubes as the origin of labyrinthus noctis and Valles marineris on mars. J. Volcanol. Geoth. Res. 277, 1–8.
Leone, G., 2017. Mangala Valles, Mars: a reassessment of formation processes based on a new geomorphological and stratigraphic analysis of the geological units. J. Volcanol. Geoth. Res. 337, 62–80.
Leone, G., 2018. Comments to "A composite mineralogical map of ganges chasma and surroundings, Valles marineris, mars" by selby cull-hearth and M. Caroline Clark (planetary and Space science 142, 1-8). Planet. Space Sci. https://doi.org/10.1016/j.pss.2018.08.002.
Leone, G., 2020. The absence of an ocean and the fate of water all over the Martian history. Earth and Space Science 7. https://doi.org/10.1029/2019EA001031.
Lepotre, M.G.A., Lamb, M.P., Williams, R.M.E., 2016. Canyon formation constraints on the discharge of catastrophic outburst floods of Earth and Mars. J. Geophys. Res. 121, 1232–1263.
Lesher, C.M., 2017. Roles of xenomelts, xenoliths, xenocrysts, xenovolatiles, residues, and skarns in the genesis, transport, and localization of magmatic Fe-Ni-Cu-PGE sulfides and chromite. Ore Geol. Rev. 90, 465–484.
Lesher, C.M., Campbell, I.H., 1993. Geochemical and fluid dynamic modeling of compositional variations in Archean komatiite-hosted nickel sulfide ores in Western Australia. Econ. Geol. 88, 804–816.
Leverington, D.W., 2004. Volcanic rilles, streamlined islands, and the origin of outflow channels on Mars. J. Geophys. Res. 109, E10011. https://doi.org/10.1029/2004JE002311.
Leverington, D.W., 2005. Evaluation of candidate crater-lake sites on Mars. In: Proc. Lunar Planet. Sci. Conf. 36th. Houston, TX, Abstract 1522.
Leverington, D.W., 2006. Volcanic processes as alternative mechanisms of landform development at a candidate crater-lake site near Tyrrhena Patera, Mars. J. Geophys. Res. 111, E11002. https://doi.org/10.1029/2004JE002382.
Leverington, D.W., 2007. Was the Mangala Valles system incised by volcanic flows? J. Geophys. Res. 112, E11005. https://doi.org/10.1029/2007JE002896.
Leverington, D.W., 2009. Reconciling channel formation mechanisms with the nature of elevated outflow systems at Ophir and Aurorae Plana, Mars. J. Geophys. Res. 114, E10005. https://doi.org/10.1029/2009JE003398.
Leverington, D.W., 2011. A volcanic origin for the outflow channels of Mars: key evidence and major implications. Geomorphology 132, 51–75.
Leverington, D.W., 2014. Did large volcanic channel systems develop on Earth during the Hadean and Archean? Precambrian Res. 246, 226–239.
Leverington, D.W., 2018. Is Kasei Valles (Mars) the largest volcanic channel in the solar system? Icarus 301, 37–57.
Leverington, D.W., 2019a. Constraints on the nature of the effusive volcanic eruptions that incised Ravi Vallis, Mars. Planet. Space Sci. 167, 54–70.
Leverington, D.W., 2019b. Formation of Ares Vallis (Mars) by effusions of low-viscosity lava within multiple regions of chaotic terrain. Geomorphology 345, 106828.
Leverington, D.W., Maxwell, T.A., 2004. An igneous origin for features of a candidate crater-lake system in western Memnonia, Mars. J. Geophys. Res. 109, E06006. https://doi.org/10.1029//2004JE002237.
Leverington, D.W., Moon, W.M., 2012. Landsat-TM-based discrimination of lithological units associated with the Purtuniq ophiolite, Quebec, Canada. Remote Sensing 4, 1208–1231.
Lucchitta, B.K., 1985. Geomorphologic evidence for ground ice on Mars. In: Klinger, J., Benest, D., Dollfus, A., Smoluchowski, R. (Eds.), Ices in the Solar System. Springer, Dordrecht, pp. 583–604.
Luo, W., Pingel, T., Heo, J., Howard, A., Jung, J., 2015. A progressive black top hat transformation algorithm for estimating valley volumes on Mars. Comput. Geosci. 75, 17–23.
Malin, M.C., Edgett, K.S., 1999. Oceans or seas in the Martian northern lowlands: high resolution imaging tests of proposed coastlines. Geophys. Res. Lett. 26, 3049–3052.
Mandon, L., Quantin-Nataf, C., Thollot, P., Mangold, N., Lozac'h, L., Dromart, G., Beck, P., Dehouck, E., Breton, S., Millot, C., Volat, M., 2020. Refining the age, emplacement and alteration scenarios of the olivine-rich unit in the Nili Fossae region, Mars. Icarus 336, 113436.
Mangold, N., Ansan, V., Baratoux, D., Costard, F., Dupeyrat, L., Hiesinger, H., Masson, Ph, Neukum, G., Pinet, P., 2008. Identification of a new outflow channel on Mars in Syrtis Major Planum using HRSC/MEx data. Planet. Space Sci. 56, 1030–1042.
Michalski, J.R., Noe Dobrea, E.Z., Niles, P.B., Cuadros, J., 2017. Ancient hydrothermal seafloor deposits in Eridania basin on Mars. Nat. Commun. 8, 15978. https://doi.org/10.1038/ncomms15978.
Michalski, J.R., Noe Dobrea, E.Z., Niles, P.B., Cuadros, J., 2018. The case for hydrothermal seafloor-type deposits in the Eridania basin on Mars. In: Proc. Lunar Planet. Sci. Conf. 49th. Houston, TX, Abstract 1757.
Milton, D.J., 1973. Water and processes of degradation in the Martian landscape. J. Geophys. Res. 78, 4037–4047.
Ming, D.W., et al., 2006. Geochemical and mineralogical indicators for aqueous processes in the Columbia Hills of Gusev crater, Mars. J. Geophys. Res. 111, E02S12. https://doi.org/10.1029/20005JE002560.
Mittlefehldt, D.W., Gellert, R., Ming, D.W., Yen, A.S., 2019. Alteration processes in Gusev Crater, Mars: volatile/mobile element contents of rocks and soils determined by the Spirit rover. In: Filiberto, J., Schwenzer, S.P. (Eds.), Chapter 11 in "Volatiles in the Martian Crust". Elsevier, pp. 329–368. https://doi.org/10.1016/B978-0-12-804191-8.00011-8.
Molina, A., de Pablo, M.Á., Hauber, E., Le Deit, L., Fernández-Remolar, D., 2014. Geology of the Ariadnes basin, NE Eridania quadrangle, mars – 1:1 million. J. Maps 10, 487–499.
Morris, R.V., et al., 2004. Mineralogy at Gusev crater from the Mössbauer spectrometer on the Spirit rover. Science 305, 833–836.
Morris, R.V., et al., 2006. Mössbauer mineralogy of rock, soil, and dust at Gusev crater, Mars: Spirit's journey through weakly altered olivine basalt on the plains and pervasively altered basalt in the Columbia Hills. J. Geophys. Res. 111, E02S13. https://doi.org/10.1029/2005JE002584.
Morris, R.V., Ruff, S.W., Gellert, R., Ming, D.W., Arvidson, R.E., Clark, B.C., Golden, D.C., Siebach, K., Klingelhofer, G., Schroder, C., Fleischer, I., Yen, A.S., Squyres, S.W., 2010. Identification of carbonate-rich outcrops on Mars by the Spirit rover. Science 329, 421–424.
Mouginis-Mark, P., 1981. Ejecta emplacement and modes of formation of Martian fluidized ejecta craters. Icarus 45, 60–76.
Mouginot, J., Pommerol, A., Beck, P., Kofman, W., Clifford, S.M., 2012. Dielectric map of the Martian northern hemisphere and the nature of plain filling materials. Geophys. Res. Lett. 39, L02202. https://doi.org/10.1029/2011GL050286.
Murase, T., McBirney, A.R., 1970. Viscosity of lunar lavas. Science 167, 1491–1493.
Murase, T., McBirney, A.R., 1973. Properties of some common igneous rocks and their melts at high temperatures. Bull. Geol. Soc. Am. 84, 3563–3592.
Niles, P.B., Michalski, J., Ming, D.W., Golden, D.C., 2017. Elevated olivine weathering rates and sulfate formation at cryogenic temperatures on Mars. Nat. Commun. 8, 998. https://doi.org/10.1038/s41467-017-01227-7.
Noe Dobrea, E.Z., Bell, J.F., Wolff, M.J., Gordon, K.D., 2003. H_2O- and OH-bearing minerals in the martian regolith: analysis of 1997 observations from HST/NICMOS. Icarus 166, 1–20.
Oberst, J., Preusker, F., Phillips, R.J., Watters, T.R., Head, J.W., Zuber, M.T., Solomon, S.C., 2010. The morphology of Mercury's Caloris basin as seen in MESSENGER stereo topographic models. Icarus 209, 230–238.
Ody, A., Poulet, F., Langevin, Y., Bibring, J.-P., Gondet, B., Carter, J., Vincendon, M., 2011. Global distribution of igneous minerals on Mars: assessing the composition of the crust. In: Proc. Lunar Planet. Sci. Conf. 42nd. Houston, TX, Abstract 2459.

Ody, A., Poulet, F., Langevin, Y., Bibring, J.-P., Gondet, B., Carter, J., 2012a. Olivine detections in the Martian northern plains with OMEGA/Mex. In: Proc. Lunar Planet. Sci. Conf. 43rd. Houston, TX, Abstract 2430.
Ody, A., Poulet, F., Langevin, Y., Bibring, J.-P., Bellucci, G., Gondet, B., Vincendon, M., Carter, J., Manaud, N., 2012b. Global maps of anhydrous minerals at the surface of Mars from OMEGA Mex. J. Geophys. Res. 117, E00J14. https://doi.org/10.1029/2012JE004117.
Ody, A., Poulet, F., Bibring, J.-P., Loizeau, D., Carter, J., Gondet, B., Langevin, Y., 2013. Global investigation of olivine on Mars: insights into crust and mantle compositions. J. Geophys. Res. 118, 234–262. https://doi.org/10.1029/2012JE004149.
Osterloo, M.M., Hamilton, V.E., Bandfield, J.L., Glotch, T.D., Baldridge, A.M., Christensen, P.R., Tornabene, L.L., Anderson, F.S., 2008. Chloride-bearing materials in the southern highlands of Mars. Science 319, 1651–1654.
Osterloo, M.M., Anderson, F.S., Hamilton, V.E., Hynek, B.M., 2010. Geologic context of proposed chloride-bearing materials on Mars. J. Geophys. Res. 115, E10012. https://doi.org/10.1029/2010JE003613.
Oze, C., Sharma, M., 2007. Serpentinization and the inorganic synthesis of H_2 in planetary surfaces. Icarus 186, 557–561.
Pajola, M., Rossato, S., Carter, J., Baratti, E., Pozzobon, R., Erculiani, M.S., Coradini, M., McBride, K., 2016. Eridania Basin: an ancient paleolake floor as the next landing site for the Mars 2020 rover. Icarus 275, 163–182.
Pan, L., Ehlmann, B.L., Carter, J., Ernst, C., 2017. The stratigraphy and history of Mars' northern lowlands through mineralogy of impact craters: a comprehensive survey. J. Geophys. Res. 122, 1824–1854.
Parker, T.J., 2000. A brief summary of the geomorphic evidence for an active surface hydrologic cycle in Mars' past. Second Int. Conf. on Mars Polar Science and Exploration, Reykjavik, Iceland. Abstract 4039.
Peplowski, P.N., Stockstill-Cahill, K., 2019. Analytical identification and characterization of the major geochemical terranes of Mercury's northern hemisphere. J. Geophys. Res. 124, 2414–2429.
Peterson, D.W., Swanson, D.A., 1974. Observed formation of lava tubes during 1970-1971 at Kilauea Volcano, Hawaii. Stud. Speleol. 2, 209–222.
Phillips, R.J., Arvidson, R.E., Boyce, J.M., Campbell, D.B., Guest, J.E., Schaber, G.G., Soderblom, L.A., 1991. Impact craters on Venus: initial analysis from magellan. Science 252, 288–297.
Plescia, J.B., 1990. Recent flood lavas in the Elysium region of Mars. Icarus 88, 465–490.
Pommerol, A., Schmitt, B., 2008. Strength of the H_2O near-infrared absorption bands in hydrated minerals: effects of particle size and correlation with albedo. J. Geophys. Res. 113, E10. https://doi.org/10.1029/2007JE003069.
Pretlow, R.W., 2013. A Geomorphological Investigation of Paleoshorelines on Mars. A Report Prepared in Partial Fulfillment of the Requirements for the Degree of Master of Science. University of Washington, Seattle, Washington.
Putzig, N.E., Mellon, M.T., 2007. Apparent thermal inertia and the surface heterogeneity of Mars. Icarus 191, 68–94.
Putzig, N.E., Mellon, M.T., Kretke, K.A., Arvidson, R.E., 2005. Global thermal inertia and surface properties of Mars from the MGS mapping mission. Icarus 173, 325–341.
Riu, L., Poulet, F., Bibring, J.-P., Gondet, B., 2019. The M^3 project: 2 – global distributions of mafic mineral abundances on Mars. Icarus 322, 31–53.
Roberts, C.E., Gregg, T.K.P., 2019. Rima Marius, the Moon: formation of lunar sinuous rilles by constructional and erosional processes. Icarus 317, 682–688.
Rogers, A.D., Christensen, P.R., Bandfield, J.L., 2005. Compositional heterogeneity of the ancient Martian crust: analysis of Ares Vallis bedrock with THEMIS and TES data. J. Geophys. Res. 110, E05010. https://doi.org/10.1029/205JE002399.
Ruesch, O., Poulet, F., Vincendon, M., Bibring, J.-P., Carter, J., Erkeling, G., Gondet, B., Hiesinger, H., Ody, A., Reiss, D., 2012. Compositional investigation of the proposed chloride-bearing materials on Mars using near-infrared orbital data from OMEGA/Mex. J. Geophys. Res. 117, E00J13. https://doi.org/10.1029/2012JE004108.
Ruff, S.W., Niles, P.B., Alfano, F., Clarke, A.B., 2014. Evidence for a noachian-aged ephemeral lake in Gusev crater, mars. Geology 42, 359–362.
Schleicher, L.S., Watters, T.R., Martin, A.J., Banks, M.E., 2019. Wrinkle ridges on Mercury and the Moon within and outside of mascons. Icarus 331, 226–237.
Schneeberger, D.M., 1989. Episodic channel activity at Ma'adim Vallis, mars. In: Proc. Lunar Planet. Sci. Conf. 20th, pp. 964–965. Houston, TX, abstract.
Schonfeld, E., 1979. Origin of Valles marineris. In: Proceedings of the 10th Lunar Science Conference, Houston, TX. Lunar and Planetary Institute, Houston, pp. 3031–3038.
Schultz, P.H., 1976. Moon Morphology. University of Texas Press, Austin, TX.
Schumm, S.A., Boyd, K.F., Wolff, C.G., Spitz, W.J., 1995. A ground-water sapping landscape in the Florida Panhandle. Geomorphology 12, 281–297.
Scott, D.H., Tanaka, K.L., 1986. Geologic map of the western equatorial region of Mars. U.S. Geol. Surv. Geol. Invest. Ser., Map I-1802-A.
Scott, D.H., Chapman, M.G., 1995. Geologic and topographic maps of the Elysium paleolake basin, Mars. U.S. Geol. Surv. Misc. Invest. Ser. Map I-2397 scale 1: 5,000,000.
Self, S., Thordarson, T., Keszthelyi, L., 1997. Emplacement of continental flood basalt lava flows. In: Mahoney, J., Coffin, F. (Eds.), Large Igneous Provinces: Continental, Oceanic and Planetary Flood Volcanism. Geophys. Monogr. Ser., 100. American Geophysical Union, Washington, D.C., pp. 381–410. https://doi.org/10.1029/GM100p0381
Sharp, R.P., Malin, M.C., 1975. Channels on mars. Geol. Soc. Am. Bull. 86, 593–609.
Shaw, H.R., Wright, T.L., Peck, D.L., Okamura, R., 1968. The viscosity of basaltic magma: an analysis of field measurements in Makaopuhi lava lake, Hawaii. Am. J. Sci. 266, 225–264.
Sholes, S.F., Montgomery, D.R., Catling, D.C., 2019. Quantitative high-resolution reexamination of a hypothesized ocean shoreline in Cydonia Mensae on Mars. J. Geophys. Res. 124, 316–336. https://doi.org/10.1029/2018JE005837.
Sklar, L., Dietrich, W.E., 1998. River longitudinal profiles and bedrock incision models: stream power and the influence of sediment supply. In: Tinkler, K.J., Wohl, E.E. (Eds.), Rivers over Rock: Fluvial Processes in Bedrock Channels, vol. 107. American Geophysical Union, Washington, DC. https://doi.org/10.1029/GM107p0237.
Smith, D., Neumann, G., Arvidson, R.E., Guinness, E.A., Slavney, S., 2003. Mars Global Surveyor Laser Altimeter Mission Experiment Gridded Data Record. NASA Planetary Data System, Greenbelt, MD., MOLA Gridded Data Record, MGS-M-MOLA-MEGDR-L3-V1.0.
Squyres, S.W., et al., 2004. The Spirit rover's Athena science investigation at Gusev crater, Mars. Science 305, 794–799.
Squyres, S.W., Arvidson, R.E., Blaney, D.L., Clark, B.C., Crumpler, L., Farrand, W.H., Gorevan, S., Herkenhoff, K., Hurowitz, J., Kusack, A., McSween, H.Y., Ming, D.W., Morris, R.V., Ruff, S.W., Wang, A., Yen, A., 2006. Rocks of the Columbia Hills. J. Geophys. Res. 111, E02S11. https://doi.org/10.1029/2005JE002562.
Squyres, S.W., Arvidson, R.E., Ruff, S., Gellert, R., Morris, R.V., Ming, D.W., Crumpler, L., Farmer, J.D., Des Marais, D.J., Yen, A., McLennan, S.M., Calvin, W., Bell, J.F., Clark, B.C., Wang, A., McCoy, T.J., Schmidt, M.E., de Souza, P.A., 2008. Detection of silica-rich deposits on Mars. Science 320, 1063–1067. https://doi.org/10.1126/science.1155429.
Staude, S., Barnes, S.J., Le Vaillant, M., 2016. Evidence of lateral thermomechanical erosion of basalt by Fe-Ni-Cu sulfide melt at Kambalda, Western Australia. Geology 44, 1047–1050.
Staude, S., Barnes, S.J., Le Vaillant, 2017. Thermomechanical erosion of ore-hosting embayments beneath komatiite lava channels: textural evidence from Kambalda, Western Australia. Ore Geol. Rev. 90, 446–464.
Stockstill-Cahill, K.R., McCoy, T.J., Nittler, L.R., Weider, S.Z., Hauck, I.I.S.A., 2012. Magnesium-rich crustal compositions on Mercury: implications for magmatism from petrologic modeling. J. Geophys. Res. 117, E00L15. https://doi.org/10.1029/2012JE004140.
Tanaka, K.L., 1986. The stratigraphy of Mars. J. Geophys. Res. 91, E139–E158.
Tanaka, K.L., Skinner, J.A., Dohm, J.M., Irwin III, R.P., Kolb, E.J., Fortezzo, C.M., Platz, T., Michael, G.G., Hare, T.M., 2014. Geologic map of mars. U.S. Geol. Surv., Sci. Invest. Map 3292.
Thomas, R.J., Rothery, D.A., Conway, S.J., Anand, M., 2014. Mechanisms of explosive volcanism on Mercury: implications from its global distribution and morphology. J. Geophys. Res. 119, 2239–2254. https://doi.org/10.1002/2014JE004692.
Thomson, B.J., Head, J.W., 2001. Utopia Basin, Mars: characterization of topography and morphology and assessment of the origin and evolution of basin internal structure. J. Geophys. Res. E10 23, 209–223, 230.
Vetere, F., Rossi, S., Namur, O., Morgavi, D., Misiti, V., Mancinelli, P., Petrelli, M., Pauselli, C., Perugini, D., 2017. Experimental constraints on the rheology, eruption, and emplacement dynamics of analog lavas comparable to Mercury's northern volcanic plains. J. Geophys. Res. 122, 1522–1538.
Vetere, F., Murri, M., Alvaro, M., Domeneghetti, M.C., Rossi, S., Pisello, A., Perugini, D., Holtz, F., 2019. Viscosity of pyroxenite melt and its evolution during cooling. J. Geophys. Res. 124, 1451–1469.
Wang, F., Bowen, B.B., Seo, J.-H., Michalski, G., 2018. Laboratory and field characterization of visible to near-infrared spectral reflectance of nitrate minerals from the Atacama Desert, Chile, and implications for Mars. Am. Mineral. 103, 197–206. https://doi.org/10.2138//am-2018-6141.
Watters, T.R., 1988. Wrinkle ridge assemblages on the terrestrial planets. J. Geophys. Res. 93 (10), 236-10,254.
Watters, T.R., Johnson, C., 2010. Lunar tectonics. In: Watters, T.R., Schultz, R.A. (Eds.), Planetary Tectonics. Cambridge University Press, New York, NY, pp. 121–182.
Watters, T.R., Nimmo, F., 2010. The tectonics of Mercury. In: Watters, T.R., Schultz, R.A. (Eds.), Planetary Tectonics. Cambridge University Press, New York, NY, pp. 15–80.
Weill, D.F., Grieve, R.A., McCallum, I.S., Bottinga, Y., 1971. Mineralogy-petrology of lunar samples. Microprobe studies of samples 12021 and 12022; viscosity of melts of selected lunar compositions. In: Proceedings of the Second Lunar Science Conference, vol. 1. The M.I.T. Press, pp. 413–430.
Weitz, C.M., Bishop, J.L., Baker, L.L., Berman, D.C., 2014. Fresh exposures of hydrous Fe-bearing amorphous silicates on Mars. Geophys. Res. Lett. 41, 8744–8751.
Wendt, L., Bishop, J.L., Neukum, G., 2013. Knob fields in the Terra Cimmeria/Terra Sirenum region of mars: stratigraphy, mineralogy and morphology. Icarus 225, 200–215.
Wieczorek, M.A., Phillips, R.J., 1999. Lunar multiring basins and the cratering process. Icarus 139, 246–259.
Wilhelms, D., 1987. The Geologic History of the Moon, vol. 1348. U.S. Geol. Surv. Prof. Pap., Washington, DC.
Williams, D.A., Kerr, R.C., Lesher, C.M., 1998. Emplacement and erosion by Archean komatiite lava flows at Kambalda: revisited. J. Geophys. Res. 103 (27), 533-27,549.
Williams, D.A., Fagents, S.A., Greeley, R., 2000. A reassessment of the emplacement and erosional potential of turbulent, low-viscosity lavas on the Moon. J. Geophys. Res. 105 (20) https://doi.org/10.1029/1999JE001220, 189-20,205.
Williams, D.A., Kerr, R.C., Lesher, M., Barnes, S.J., 2001. Analytical/numerical modeling of lava emplacement and thermal erosion at Perseverance, Western Australia. J. Volcanol. Geoth. Res. 110, 27–55.
Williams, D.A., Kerr, R.C., Lesher, C., 2011. Mathematical modeling of thermomechanical erosion beneath Proterozoic komatiitic basaltic sinuous rilles in the Cape Smith Belt, New Quebec, Canada. Miner. Deposita 8, 943–958. https://doi.org/10.1007/s00126-011-0364-5.
Wilson, J.H., Mustard, J.F., 2013. Exposures of olivine-rich rocks in the vicinity of ares Vallis: implications for noachian and hesperian volcanism. J. Geophys. Res. 118, 916–929.

Wilson, L., Head III, J.W., 2002. Tharsis-radial graben systems as the surface manifestation of plume-related dike intrusion complexes: models and implications. J. Geophys. Res. 107, E8. https://doi.org/10.1029/2001JE001593.

Wordsworth, R.D., 2016. The climate of early Mars. Annu. Rev. Earth Planet Sci. 44, 381–408.

Yen, A.S., Morris, R.V., Clark, B.C., Gellert, R., Knudson, A.T., Squyres, S., Mittlefehldt, D.W., Ming, D.W., Arvidson, R., McCoy, T., Schmidt, M., Hurowitz, J., Li, R., Johnson, J.R., 2008. Hydrothermal processes at Gusev crater: an evaluation of Paso Robles class soils. J. Geophys. Res. 113, E06S10. https://doi.org/10.1029/2007JE002978.

You, J., Kauhanen, K., Raitala, J., 1995. Fractal properties of crater ejecta outlines on Venus. Earth, Moon, and Planets 71, 9–31.

Zavialov, P.O., Kostianoy, A.G., Emelianov, S.V., Ni, A.A., Ishniyazov, D., Khan, V.M., Kudyshkin, T.V., 2003. Hydrographic survey in the dying aral sea. Geophys. Res. Lett. 30 https://doi.org/10.1029/2003GL017427.

Zhang, F., Zhu, M.-H., Zou, Y.L., 2016. Late stage Imbrium volcanism on the Moon: evidence for two source regions and implications for the thermal history of Mare Imbrium. Earth Planet Sci. Lett. 445, 13–27.